DIMENSIONLESS PRESSURE AND PRESSURE DERIVATIVE RESPONSES OF A HORIZONTAL WELL COMPLETED IN A RESERVOIR WITH INCLINED IMPERMEABLE BOUNDARIES

BY

ENOFE GABRIEL OSASERE

ENG1805537

A PROJECT REPORT PRESENTED TO THE

DEPARTMENT OF PETROLEUM ENGINEERING

UNIVERSITY OF BENIN

IN PARTIAL FULFILMENT FOR THE AWARD OF

BACHELOR OF ENGINEERING DEGREE IN

PETROLEUM ENGINEERING

APRIL, 2024

CERTIFICATION

This is to certify that this project work was carried out by ENOFE GABRIEL OSASERE of the Department of Petroleum Engineering, Faculty of Engineering, University of Benin, in partial fulfilment for the award of Bachelor in Engineering (B.Eng.) degree in Petroleum Engineering.

________________________________ ____________________

PROF. E.S. ADEWOLE **DATE**

(PROJECT SUPERVISOR)

ENGR TAIWO, O. A **DATE**

(PROJECT CO-ORDINATOR)

ENGR. DR. S.A. IGBINERE **DATE**

(HEAD OF DEPARTMENT)

PROF. S.O. ISEHUNWA, PhD **DATE**

(EXTERNAL EXAMINER)

DEDICATION

I dedicate this project to God Almighty for His bountiful grace and strength upon my life to go through my course duration and also in dedication to Mum Mrs. Enofe Tina Osahenoma for all her effort put into making me who I am today.

ACKNOWLEDGEMENT

I am so grateful to Almighty God for empowering me to successfully complete this project and for His grace all through the duration of my course.

I am grateful to Dr. S.A Igbinere the H.O.D of the Department of Petroleum Engineering, University of Benin, Nigeria for his immense contribution and support to provide a conducive environment for me to carry out this study effectively. I would also like to thank my siblings Jennifer Enofe, and Vera Enofe for their support, advice, encouragement and prayers all through the duration of my course.

I specially appreciate my supervisor Prof. E.S. Adewole for his selfless effort, patience, support and huge impact in making sure this project was an enjoyable and an eventful one.

More so, this project would not be a success without the help of my friends Bolaji and Patrick for their emotional support and encouragement and my colleagues for their constant help in the duration of my course.

ABSTRACT

This study investigates the dimensionless pressure and pressure derivative responses of a horizontal well within a reservoir characterized by inclined impermeable boundaries. Horizontal wells have gained prominence in recent years due to their potential to enhance hydrocarbon recovery from unconventional reservoirs. However, their behavior in reservoirs with non-conventional boundaries remains less understood.

In this research, we employ analytical and numerical techniques to model the pressure and pressure derivative responses of a horizontal well situated in such a reservoir. By utilizing dimensionless analysis, we aim to generalize the findings across various reservoir conditions and well geometries. The influence of inclined impermeable boundaries on well performance is examined, considering factors such as boundary angle, reservoir anisotropy, and wellbore inclination.

Through comprehensive simulations and sensitivity analyses, key insights into the behavior of horizontal wells in reservoirs with inclined impermeable boundaries are elucidated. The derived dimensionless pressure and pressure derivative solutions provide valuable tools for reservoir engineers to optimize well design and production strategies in such challenging environments.

This study contributes to a deeper understanding of the complex interactions between wellbore geometry, reservoir boundaries, and fluid flow dynamics, paving the way for more efficient exploitation of hydrocarbon resources in unconventional reservoirs.

LIST OF TABLES

LIST OF FIGURES

TABLE OF CONTENTS

CHAPTER ONE

1.0 INTRODUCTION

1.1 BACKGROUND OF STUDY

Horizontal well completions have become increasingly popular in the oil and gas industry due to their ability to access larger reservoir areas and enhance hydrocarbon recovery. However, the behavior of such wells within inclined sealing boundaries presents unique challenges and opportunities. Understanding the dimensionless pressure and derivative responses of horizontal wells in this context is crucial for optimizing reservoir management strategies.

The effective exploitation of hydrocarbon reservoirs, particularly unconventional resources, demands a comprehensive understanding of well performance within complex geological formations. Horizontal wells, increasingly prevalent in modern drilling operations, present unique challenges and opportunities, especially when completed within formations bounded by inclined sealing interfaces.

This project aims to investigate the dimensionless pressure and derivative responses of horizontal wells positioned within such inclined sealing boundaries. By employing analytical and numerical methods, we seek to elucidate the behaviors and characteristics of pressure distribution and derivative signatures under varying reservoir and wellbore conditions.

1.2 STATEMENT OF THE PROBLEM

The objective of this project is to analyze and model the dimensionless pressure and pressure derivative responses of a horizontal well within a reservoir featuring inclined impermeable boundaries. This study aims to investigate the impact of reservoir geometry on well performance, considering the influence of inclined impermeable boundaries on pressure behavior. Through rigorous analysis, the project seeks to provide insights into the complex dynamics of horizontal well completions in reservoirs with non-traditional boundaries, contributing to a deeper understanding of reservoir engineering and enhancing the optimization of hydrocarbon recovery strategies.

1.3 AIM AND OBJECTIVES

The main aim of this project is to develop an analytic model to investigate dimensionless pressure and pressure derivative for horizontal wells completed within a sealing boundary. The specific objectives include:

1. Investigation of the influence of reservoir heterogeneity and well configuration on pressure distribution.
2. Perform full reservoir characterization.
3. Analyze the effect of near wellbore conditions on well performance.
4. Investigate the effects of well location and design on well performance.
5. Validate the developed models through comparison of result with real-time data.

1.4 SIGNIFICANCE OF THE STUDY

Findings of this research hold significant implications for reservoir management strategies, wellbore design optimization, and production forecasting in unconventional reservoirs. By enhancing our understanding of pressure dynamics in horizontally drilled wells within complex geological settings, this project aims to contribute to the advancement of efficient and sustainable hydrocarbon recovery practices.

The findings of this research will contribute to the optimization of horizontal well completions in reservoirs with inclined sealing boundaries, ultimately enhancing hydrocarbon recovery and maximizing economic returns for operators in the oil and gas industry. Additionally, the insights gained from this study can inform future reservoir management strategies and guide decision-making processes in similar geological settings.

1.5 LIMITATIONS

The study may assume simplified reservoir geometries to facilitate numerical simulations and analytical solutions, potentially limiting the direct applicability of the findings to complex geological structures.

Certain assumptions may be made during the dimensionless analysis, such as selection of characteristic length and time scales, which could introduce uncertainties in the interpretation of dimensionless pressure responses.

Validation of numerical and analytical models against field data may be challenging due to limited access to real-world data from horizontal wells completed within inclined sealing boundaries.

CHAPTER TWO

2.0 LITERATURE REVIEW

2.1 INTRODUCTION TO HORIZONTAL WELL IN RESERVOIR ENGINEERING

A horizontal well is a wellbore that is drilled at an angle, typically greater than 80 degrees from vertical, in order to intersect a reservoir horizontally. This drilling technique has gained popularity in reservoir engineering due to its numerous advantages and wide range of applications. One of the main advantages of horizontal wells is their increased contact area with the reservoir. By extending the wellbore horizontally, the well is exposed to a larger volume of the reservoir, resulting in improved production rates. This increased contact area allows for enhanced fluid flow and greater access to oil or gas reserves, ultimately maximizing the recovery from the reservoir.

Horizontal wells also have the ability to access bypassed or previously untapped areas of the reservoir. By drilling perpendicular to the natural fractures or bedding planes, these wells can intersect multiple zones within the reservoir, which may have been inaccessible with vertical wells. This enables the exploitation of additional resources and can lead to significant increases in production. Another advantage of horizontal wells is their ability to control the flow of fluids in the reservoir. By placing completion equipment, such as packers and sliding sleeves, at various points along the horizontal section, engineers can selectively control the production from different zones. This allows for better reservoir management and the optimization of production rates from specific intervals, which can be especially beneficial in heterogeneous reservoirs.

Horizontal wells are also effective in mitigating certain reservoir challenges. They can help overcome coning and water or gas breakthrough issues by distributing the production over a larger area. Additionally, these wells can be used in conjunction with various reservoir stimulation techniques, such as hydraulic fracturing or acidizing, to improve well productivity and enhance reservoir performance.

In terms of applications, horizontal wells are commonly used in tight or unconventional reservoirs, where the permeability is low and the hydrocarbons are tightly trapped. The horizontal drilling technique enables the well to intersect more of these low-permeability zones, enhancing the overall productivity of the reservoir. Furthermore, horizontal wells are extensively utilized in offshore drilling operations. By drilling horizontally beneath the seabed, operators can access reservoirs located far offshore from a single drilling platform, reducing costs and environmental impact.

Here are some of the key benefits of using horizontal wells:

- **Increased reservoir contact:** A horizontal wellbore can intersect a much larger volume of the reservoir compared to a vertical well, which can significantly increase well productivity. This is especially beneficial in thin reservoirs or those with a large areal extent.

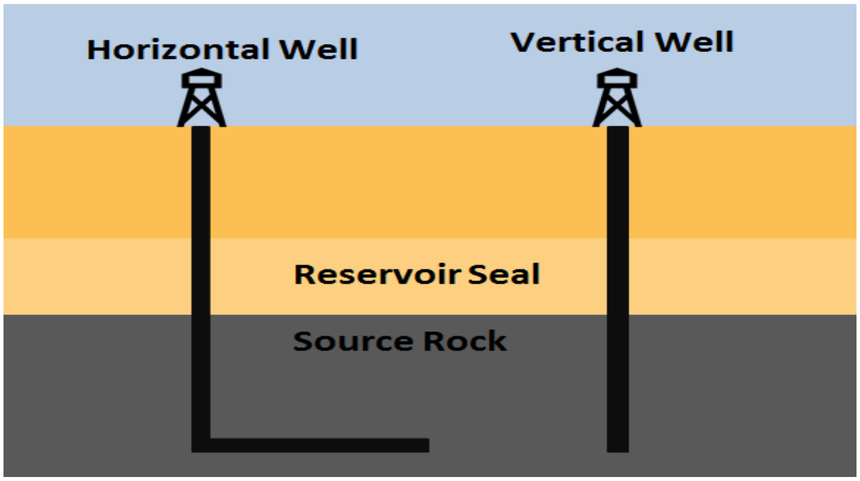

Figure 2. 1: **Horizontal well vs vertical well reservoir contact**

- **Reduced coning:** Coning refers to the phenomenon where water or gas, which are typically less viscous than oil, can flow more easily and breakthrough into the wellbore prematurely, reducing oil recovery. Horizontal wells can help mitigate this problem by providing a larger drainage area and reducing the pressure drawdown around the wellbore.
- **Improved recovery in heterogeneous reservoirs:** Reservoirs can be naturally heterogeneous, meaning that the rock properties (such as porosity and permeability) can vary significantly throughout the formation. Horizontal wells can be specifically targeted to intersect zones of higher permeability, leading to improved oil recovery.
- **Gravity drainage:** In low-pressure reservoirs, horizontal wells can be drilled in the upper part of the reservoir to take advantage of gravity drainage. This allows the oil to flow down into the wellbore due to gravity, improving recovery efficiency.

However, there are also some challenges associated with drilling and operating horizontal wells:

- **Higher drilling costs:** Drilling horizontal wells is significantly more complex and expensive compared to drilling vertical wells.
- **Completion challenges:** Completing horizontal wells requires specialized tools and techniques, which can add to the cost and complexity of the operation.
- **Reservoir characterization:** Accurate reservoir characterization is critical for designing and operating horizontal wells effectively.

2.1.1 Advantages of Horizontal Well Completions Compared to Vertical Wells

1. **Increased Contact with Reservoir**:

   - Horizontal wells have a much longer lateral section compared to vertical wells. This extended reach allows for greater contact with the reservoir, exposing a larger surface area to the productive zone.

   - By intersecting multiple layers of the reservoir or targeting specific zones with high permeability, horizontal wells can efficiently drain hydrocarbons from a larger volume of the reservoir.

2. **Improved Reservoir Drainage and Sweep Efficiency**:

   - The horizontal trajectory of the wellbore enables more uniform fluid drainage along the reservoir's horizontal axis. This enhances sweep efficiency by reducing the likelihood of bypassed oil and improving the displacement of hydrocarbons towards the wellbore.

   - Horizontal wells are particularly effective in reservoirs with thin pay zones, heterogeneous formations, or low permeability, where vertical wells may struggle to adequately access and produce hydrocarbons.

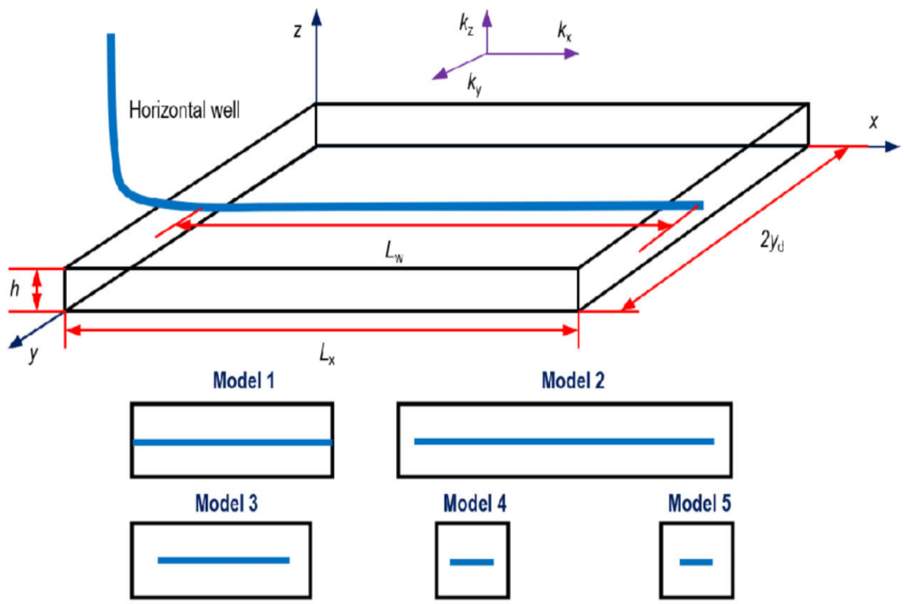

Figure 2. 2**: Schematic of Horizontal Well Drainage**

3. **Enhanced Well Performance and Productivity**:

    - Horizontal well completions typically result in higher initial production rates and sustained flow rates compared to vertical wells. This is attributed to the larger drainage area and increased reservoir contact, which allows for greater fluid influx and improved reservoir performance.

    - The longer production interval of horizontal wells minimizes the drawdown pressure near the wellbore, reducing the risk of formation damage and improving well productivity over the life of the well.

4. **Reservoir Management and Improved Sweep Efficiency**:

    - Horizontal wells offer greater flexibility in reservoir management strategies, such as water or gas injection for enhanced oil recovery (EOR) purposes. The horizontal orientation allows for more efficient distribution of injected fluids and better reservoir sweep efficiency.

- By controlling injection and production rates along different sections of the wellbore, operators can optimize fluid displacement and enhance oil recovery from targeted zones within the reservoir.

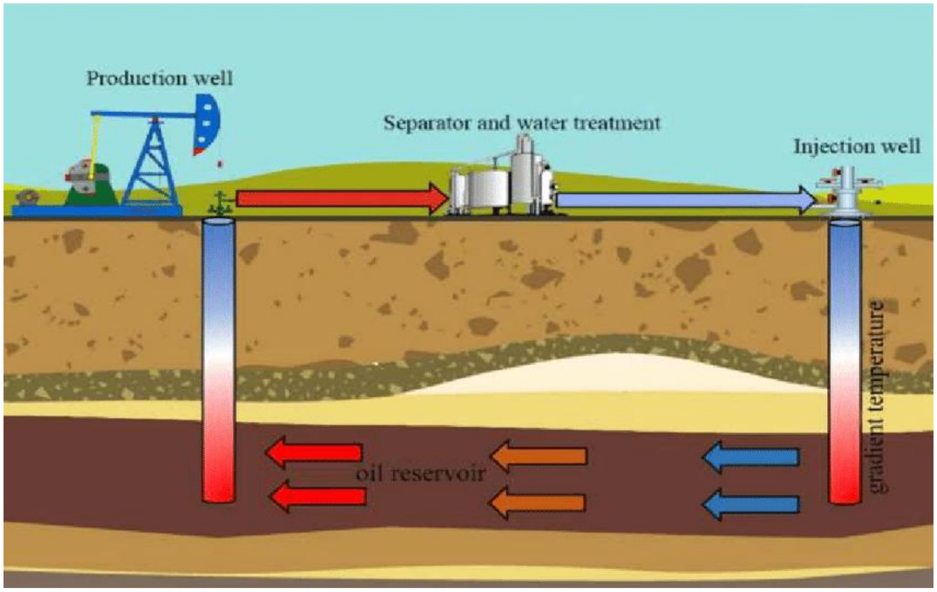

Figure 2. 3**: Water Injection in Horizontal Well**

5. **Reduced Environmental Footprint and Surface Disturbance**:

- Horizontal wells require fewer drilling locations to access the same volume of hydrocarbons compared to vertical wells. This reduces surface footprint, minimizes land disturbance, and lowers environmental impact.

- Consolidating multiple wellbores into a single drilling pad reduces the need for extensive infrastructure, such as access roads and well pads, resulting in cost savings and reduced surface disruption.

6. **Mitigation of Water or Gas Coning**:

- In reservoirs prone to water or gas coning, horizontal wells can be strategically positioned to mitigate coning effects by intersecting the hydrocarbon zone at a distance from the water or gas contact. This allows for better control over fluid production and reservoir management, minimizing the risk of early water or gas breakthrough.

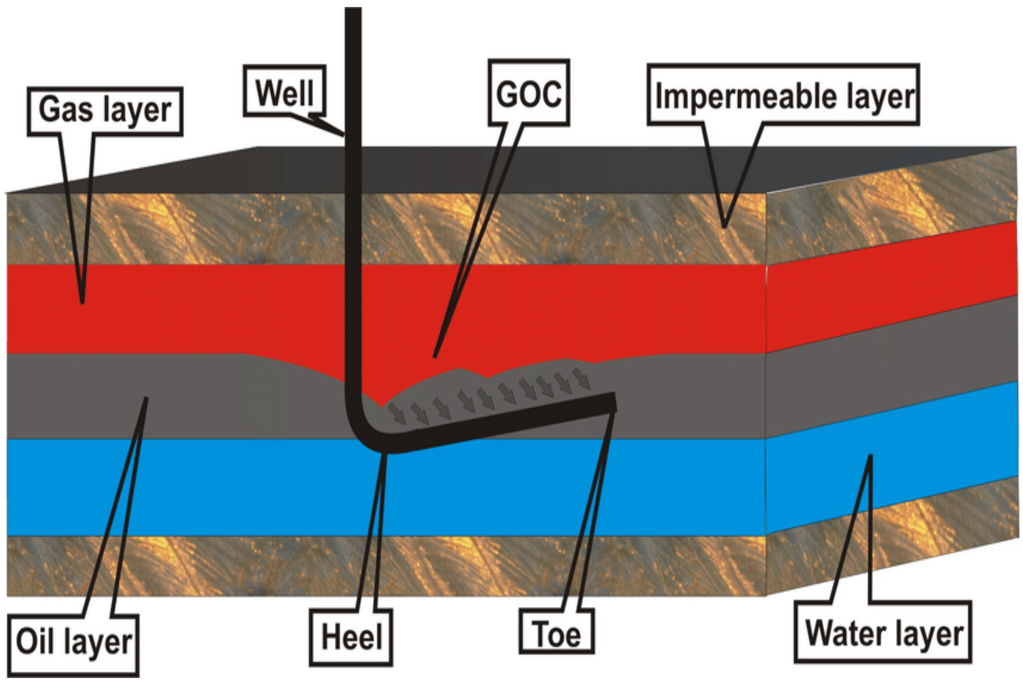

***Figure 2. 4*: Coning Mitigation - Horizontal Well Placement**

Overall, horizontal well completions offer significant advantages in maximizing hydrocarbon recovery, optimizing reservoir performance, and reducing environmental impact compared to vertical wells. These benefits make horizontal wells a preferred choice for many oil and gas operators, particularly in challenging reservoir environments and unconventional resource plays.

2.1.2 Importance of Pressure Derivatives for Optimizing Horizontal Well Performance

Understanding pressure behavior and pressure derivatives is crucial for optimizing the performance of horizontal wells. Here are key reasons why:

1. **Reservoir Characterization**:
    - Pressure behavior and pressure derivatives provide valuable insights into reservoir properties such as permeability, reservoir boundaries, and fluid flow mechanisms. Analyzing pressure transient data helps in characterizing the reservoir and identifying key parameters that influence well performance.
2. **Well Placement and Completion Design**:
    - Pressure behavior and pressure derivatives aid in determining optimal well placement and completion design. By analyzing pressure responses, engineers can identify areas of high permeability, stratigraphic heterogeneities, and barriers to fluid flow, guiding decisions on horizontal well trajectory, lateral length, and completion intervals.
3. **Production Forecasting and Reservoir Management**:
    - Pressure transient analysis facilitates production forecasting and reservoir management. Understanding pressure behavior over time helps predict well productivity, estimate ultimate recovery, and optimize production strategies such as production rates, choke sizes, and artificial lift methods.

4. **Identification of Reservoir Boundaries and Fluid Contacts**:

   - Pressure behavior provides information about reservoir boundaries, fluid contacts, and compartmentalization. Pressure derivative analysis aids in identifying sudden changes in reservoir properties, discontinuities, or fluid interfaces, which are indicative of faults, fractures, or compartmentalized zones within the reservoir.

5. **Monitoring Reservoir Performance and Well Integrity**:

   - Continuous monitoring of pressure behavior and pressure derivatives allows for early detection of reservoir depletion, fluid influx, or changes in well performance. Anomalies in pressure responses may indicate reservoir connectivity issues, water or gas breakthrough, or integrity problems in the wellbore.

2.2 RESERVOIR BOUNDARIES AND THEIR INFLUENCE ON WELL PERFORMANCE

Reservoir boundaries, particularly inclined impermeable boundaries, significantly influence fluid flow dynamics by creating preferential flow paths, compartmentalizing the reservoir, and impacting pressure distribution, which necessitates careful consideration for optimizing reservoir management and maximizing hydrocarbon recovery.

Reservoir boundaries play a crucial role in dictating fluid flow dynamics within the reservoir. The presence of inclined impermeable boundaries, in particular, introduces additional complexities compared to simpler geometries like spherical or rectangular reservoirs. Here's how they impact the flow:

1. Channeling and preferential flow paths:

- Inclined boundaries can create channeling effects, where the fluid preferentially flows along specific paths instead of uniformly throughout the reservoir. This can occur due to:
  - **Pressure gradients:** As fluid flows towards the production well, pressure depletes near the wellbore, creating a pressure gradient that drives the flow. Inclined boundaries can influence the direction of this gradient, directing flow towards certain areas and away from others.
  - **Permeability variations:** The reservoir rock itself may have varying permeability along different directions. Inclined boundaries can intersect these variations, further influencing the channeling effect.

2. Early breakthrough and uneven pressure distribution:

- Due to channeling, fluid might reach the production well unevenly. This can lead to early breakthrough of fluids with lower viscosity or higher mobility, impacting the overall recovery efficiency.
- The pressure distribution within the reservoir becomes uneven, with higher pressure zones near the impermeable boundaries and lower pressure zones closer to the wellbore. This non-uniform pressure distribution can affect the driving force for fluid flow and impact production rates.

3. Impact on wellbore placement and production strategies:

- Understanding the impact of inclined boundaries is crucial for optimizing wellbore placement. By strategically placing wells in areas with favorable flow paths, engineers can maximize production efficiency and minimize the negative effects of channeling.

- Reservoir with inclined boundaries may require specialized production strategies compared to simpler geometries. Techniques like infill drilling (placing additional wells), horizontal drilling, or hydraulic fracturing might be employed to improve sweep efficiency and access fluids trapped in less accessible regions.

4. Increased complexity in modeling and reservoir characterization:

- The presence of inclined boundaries makes reservoir modeling and characterization more complex. Advanced numerical methods and simulations are often required to accurately predict fluid flow behavior and optimize production strategies.

Overall, inclined impermeable boundaries introduce challenges in managing fluid flow dynamics within a reservoir. However, with proper understanding and utilization of appropriate techniques, engineers can still achieve efficient and optimized production from such reservoirs.

2.2.1 Effects of Boundary Pressure in Reservoirs with Complex Geometries

Boundary effects have a profound influence on pressure transient responses observed in wells completed in reservoirs with complex geometries by altering fluid flow dynamics, creating non-uniform pressure distributions, and affecting well performance. These effects include:

1. **Flow Channeling and Coning**:
    - In reservoirs with complex geometries, such as inclined impermeable boundaries or fault zones, flow channeling and coning phenomena may occur, where fluids migrate preferentially along high-permeability pathways or towards wellbores due to pressure differentials, resulting in non-uniform pressure distributions and early breakthroughs.
2. **Reservoir Compartmentalization**:
    - Complex reservoir geometries, including faults, stratigraphic layers, or pinch-outs, can compartmentalize the reservoir into distinct flow units with limited communication between them. This compartmentalization leads to localized pressure variations, delayed pressure responses, and challenges in predicting well performance.
3. **Barrier Effects and Pressure Redistribution**:
    - Impermeable boundaries act as barriers to fluid flow, causing pressure differentials and redistribution of fluids within the reservoir. The presence of inclined boundaries can induce gravity-driven fluid movement, influencing pressure transient responses and well productivity.
4. **Fluid Flow Heterogeneity**:
    - Variations in reservoir permeability, porosity, and fluid properties across complex geometries result in heterogeneous fluid flow patterns. This heterogeneity affects

pressure transient behavior, leading to delayed pressure responses, irregular pressure buildup or decline curves, and challenges in interpretation.

5. **Influence on Well Testing and Interpretation**:

   - Boundary effects complicate well testing and pressure transient analysis in reservoirs with complex geometries, requiring sophisticated interpretation techniques to account for non-uniform pressure distributions, transient flow regimes, and reservoir connectivity issues.

2.2.2 Relevant Literature Reviews on Reservoir Boundary Effects in Various Geological Settings

Reviewing literature on reservoir boundary effects in various geological settings provides insights into the diverse factors influencing fluid flow dynamics, pressure behavior, and reservoir performance. Here's a summary of relevant literature across different geological settings:

Geological Setting	**Relevant Literature**
Clayey Reservoirs	Lashkaripour and Yarmohammadtooski (2018)
	- Impact of clayey boundaries on fluid flow dynamics
	- Influence on pressure distribution and compartmentalization
Fractured Reservoirs	Zhang et al. (2019)
	- Boundary effects in fractured reservoirs

	- Importance of characterizing fracture networks
Unconventional Reservoirs	Zeng et al. (2020)
	- Boundary effects in unconventional reservoirs
	- Influence of natural fractures and faults
Faulted Reservoirs	Chen et al. (2017)
	- Boundary effects in faulted reservoirs
	- Role of faults in compartmentalizing the reservoir
Deepwater Reservoirs	Li et al. (2018)
	- Boundary effects in deepwater reservoirs
	- Impact of salt diapirs and subsalt structures
Carbonate Reservoirs	Al-Maamari et al. (2019)
	- Boundary effects in carbonate reservoirs
	- Influence of faults, fractures, and karst features
Hydrocarbon Migration in Sedimentary Basins	Wang et al. (2021)
	- Boundary effects on hydrocarbon migration
	- Influence of faults, seals, and stratigraphic traps
Reservoir Modeling and Simulation	Xie et al. (2020)

	- Numerical modeling of boundary effects in reservoir simulation
	- Computational approaches for assessing reservoir connectivity

Table2. 1 **Relevant literature across different geological settings and their respective focus areas on boundary effects in reservoirs.**

2.3 DIMENSIONLESS PRESSURE AND PRESSURE DERIVATIVE ANALYSIS

2.3.1 Dimensionless Pressure Analysis

- Dimensionless pressure, often denoted as pD, is a normalized form of the pressure observed during well testing. It is expressed as the ratio of the difference between the actual pressure and initial pressure to the pressure change at a particular time: $pD = \Delta p(t) - pi$ where:
    - $p(t)$ is the pressure at time t,
    - pi is the initial pressure,
    - Δp is the pressure change during the test.
- By plotting dimensionless pressure against dimensionless time (tD), which is the ratio of time to a characteristic time scale, typically the time at which the pressure disturbance reaches the boundary of the reservoir, engineers can analyze the reservoir's behavior independent of its specific properties (such as size, shape, and permeability).
- Dimensionless pressure analysis helps in identifying the flow regimes (such as radial flow, linear flow, or boundary-dominated flow) occurring during the transient test and estimating key reservoir parameters like permeability, skin factor, and reservoir boundaries.

2.3.2 Dimensionless Pressure Derivative Analysis

- The pressure derivative, denoted as $\partial t \partial p$, represents the rate of change of pressure with respect to time. In well testing, the pressure derivative is often used because it enhances the interpretation of transient pressure data, particularly in distinguishing between different flow regimes.
- Pressure derivative analysis involves plotting the pressure derivative against dimensionless time. This plot can provide valuable information about the reservoir's heterogeneity, boundaries, and fluid properties.
- The shape and behavior of the pressure derivative curve at different times provide insights into the dominant flow mechanisms occurring in the reservoir. For instance, the slope of the curve at early times indicates the presence of radial flow, while the late-time behavior reflects boundary-dominated flow.
- Analyzing the pressure derivative curve allows engineers to estimate reservoir parameters more accurately and make informed decisions regarding reservoir management and production optimization.

In summary, dimensionless pressure and pressure derivative analysis are powerful techniques in well testing and reservoir characterization, enabling engineers and geoscientists to extract valuable information about reservoir behavior, estimate key parameters, and optimize production strategies.

CHAPTER THREE

METHODOLOGY

3.1. INTRODUCTION

Dimensionless pressure expressions for unsteady state, or infinite-acting, or radial flow period solution for vertical and horizontal wells (as solution to oil flow diffusivity equation)

For a horizontal well,

$$P_D = -\frac{\propto}{4L_D}\left[E_i\left(\frac{r_{wD}^2}{4t_D/C_D}\right)\right] + s \qquad 1$$

C_D dimensionless wellbore storage

L_D dimensionless well length

r_{wD} dimensionless well radius

P_D dimensionless pressure

t_D dimensionless time

S wellbore skin

r_D dimensionless radius

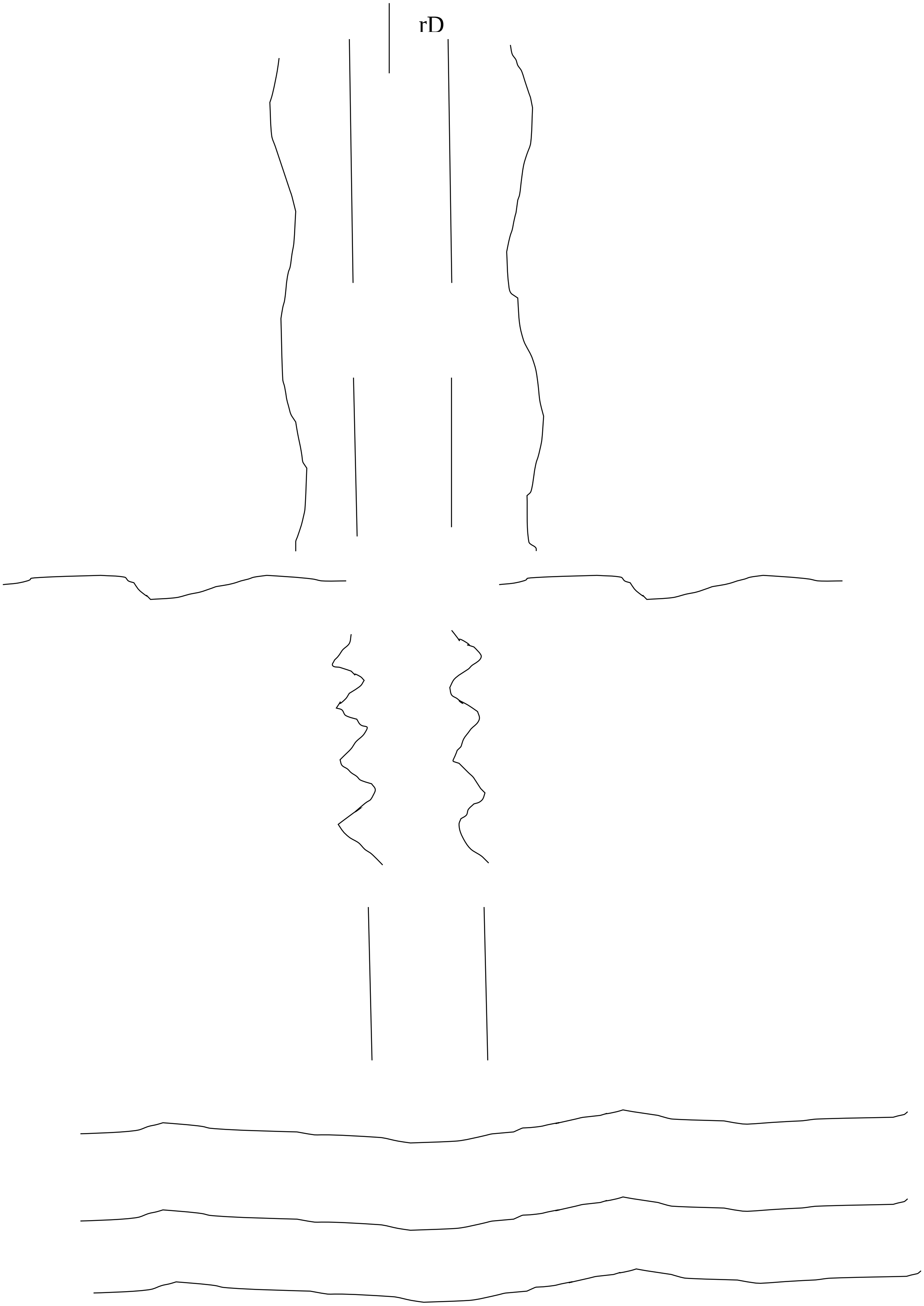

rWD, zwD, zD

r_{wD}= Z_D - Z_{wD}

Z_D dimensionless vertical well position

Z_{wD} dimensionless well stand-off well position

Alpha is 2 (infinite conductivity or uniform flux)

Ei exponential integral function

Other solutions to the diffusivity equation (mentioned briefly)

- Pseudosteady (quasi or semi) state flow period solution (caused by sealing boundaries (no-flow boundaries))
- Steady state flow period solution
- Transition flow period

Infinite-acting reservoir flow period is a flow period when no external boundary effect distorts flow streamlines the well feels that no external reservoir boundary exists. This is most preferred flow period

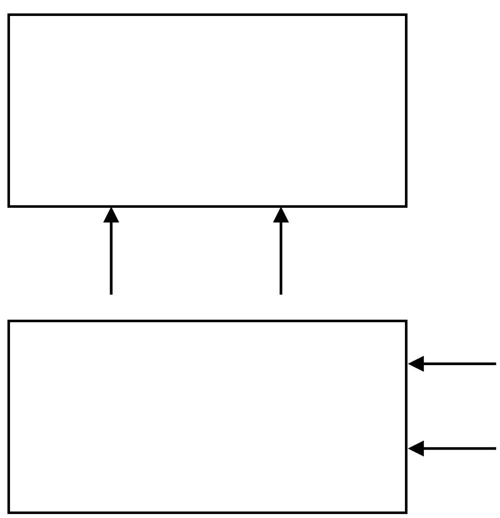

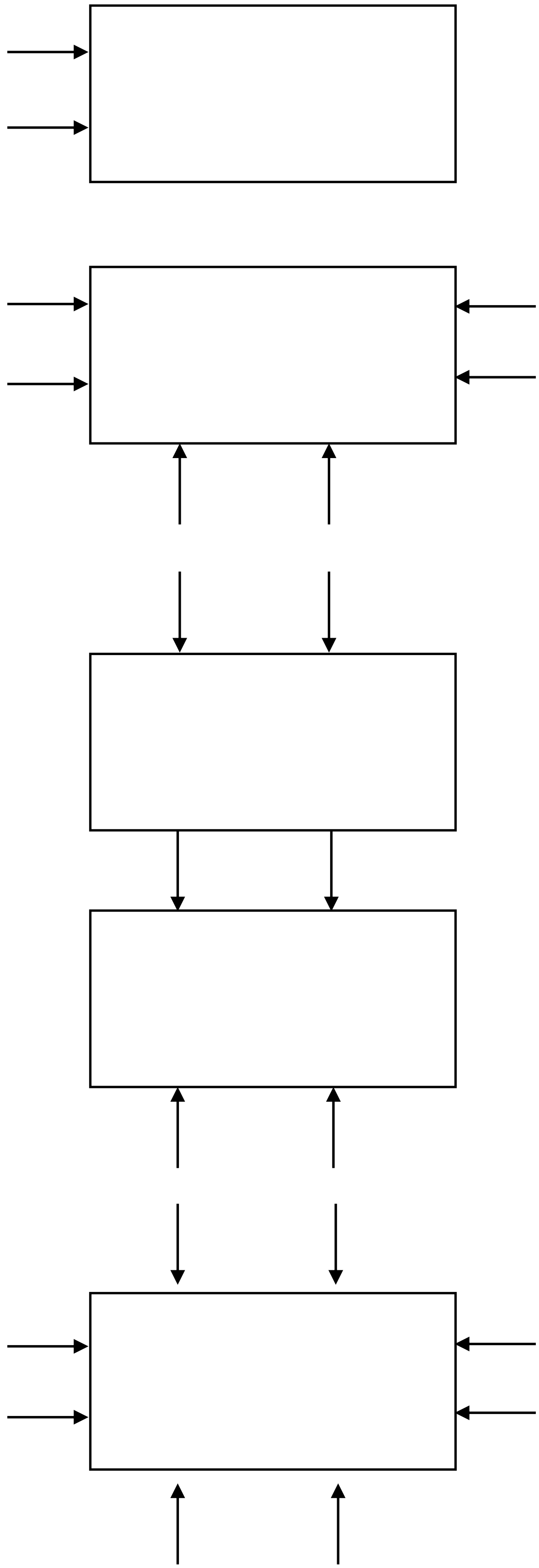

Flow periods can be recognized by

- Use of pressure gradients on
- Dimensionless pressure versus dimensionless time plots
- Dimensionless pressure derivatives plots

Use of Ei function

Calculate x, where is

$$x = \frac{948\phi\mu c_t r^2}{kt}$$

If x is less or equal to 0.01, then, Ei(x) = ln(1.781x)

For all r = r_w, x is mostly less than or equal to 0.01.

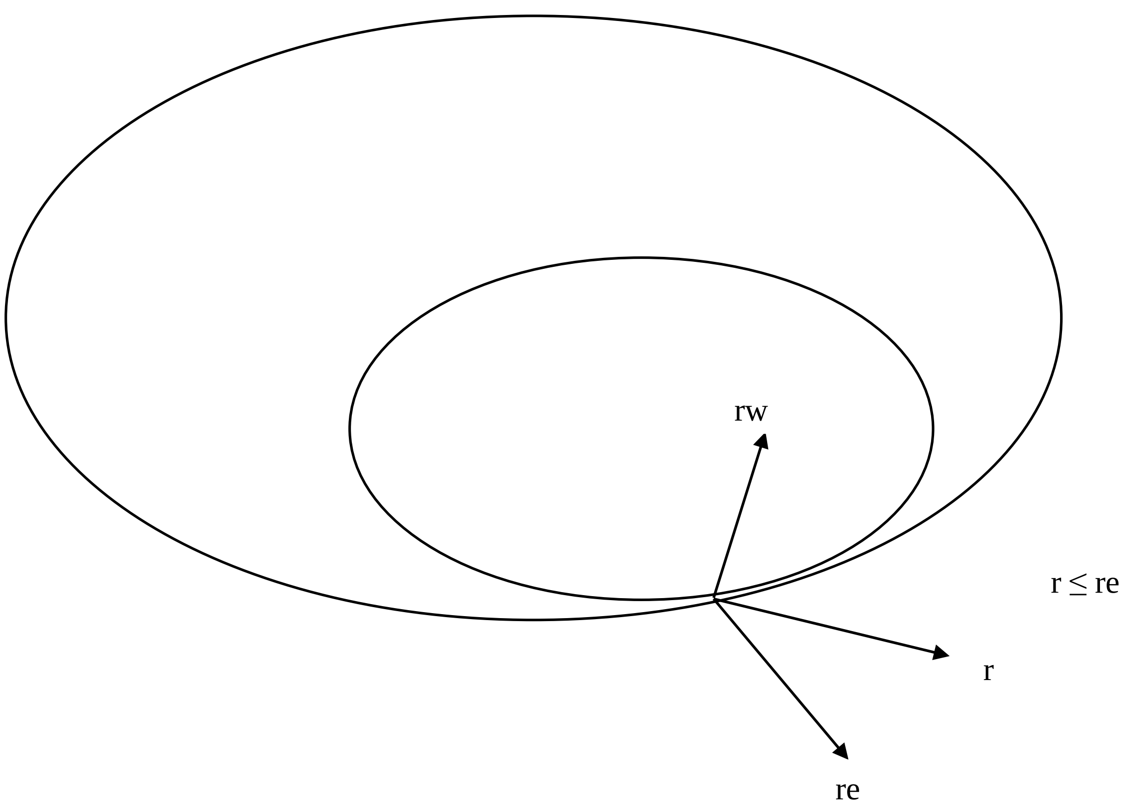

Superposition in single wells

For example, if a well produces oil at the rate of q1 for time t1 and the rate is changed to q2 to date, then, at time t greater than t1 and t2, the total pressure drop in the well to date is pressure due to rate q1 for time t +pressure drop due to rate (q2-q1) for time (t-t1).

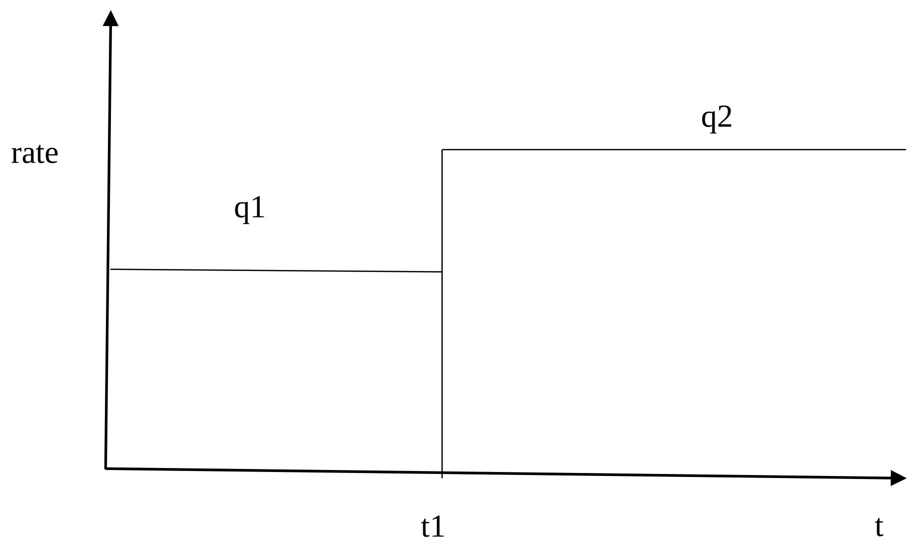

$$\Delta P_T = -\frac{70.6q\mu B}{kh}\left[Ei\left(\frac{948\emptyset\mu C_t r_w^2}{kt}\right)-2s\right] - \frac{70.6(q_2-q_1)\mu B}{kh}\left[Ei\left(\frac{948\emptyset\mu C_t r_w^2}{k(t-t_1)}\right)-2s\right] \quad 2$$

Superposition in multiple wells q11

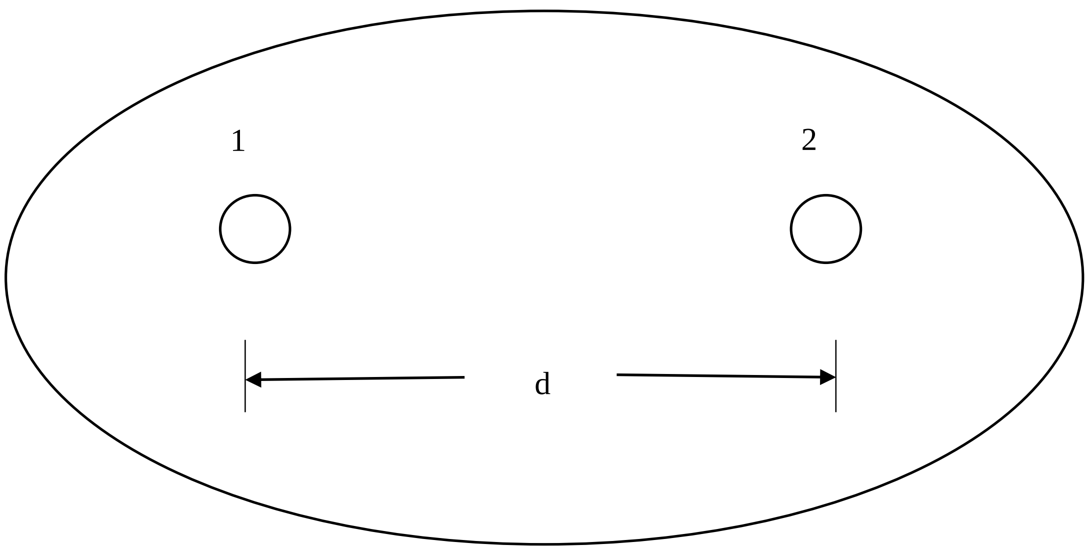

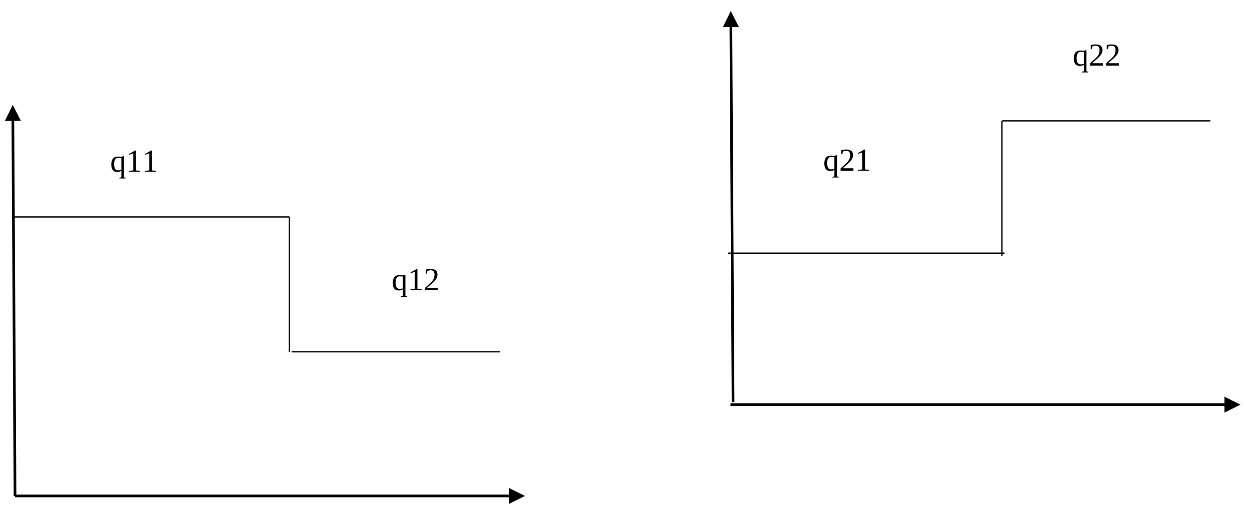

$t > t_1$

If the two wells are communication, then total pressure drop in Well 1

$\Delta P_{T,1} = \Delta P_{1,1} + \Delta P_{1,2}$

$$\Delta P_{1,1} = -\frac{70.6 q_{11} \mu B}{kh}[\mathrm{Ei}(\frac{948\emptyset\mu C_t r_{w1}^2}{kt}) - 2S_1] - \frac{70.6(q_{12}-q_{11})\mu B}{kh}[\mathrm{Ei}(\frac{948\emptyset\mu C_t r_w^2}{k(t-t_1)}) - 2S_1] \qquad 3$$

$$\Delta P_{1,2} = -\frac{70.6 q_{21} \mu B}{kh}[\mathrm{Ei}(\frac{948\emptyset\mu C_t d^2}{kt}) - 2S_1] - \frac{70.6(q_{22}-q_{21})\mu B}{kh}[\mathrm{Ei}(\frac{948\emptyset\mu C_t d^2}{k(t-t_1)}) - 2S_1] \qquad 4$$

In the superposition principle, only pressure drops are added

It can be shown that pressure drops can be replaced with dimensionless pressure drops. That is,

$$\Delta p_T = \Delta p_{1,1} + \Delta p_{1,2} + \Delta p_{1,3} + \ldots..$$

Can be written as

$$p_{D,T} = p_{D1,1} + p_{D1,2} + p_{D1,3} + \ldots..$$

3.2. DERIVATION OF MATHEMATICAL MODEL

Definition of dimensionless parameters

$$\text{Dimensionless pressure} = p_D = \frac{kh\Delta p}{141.2 q\mu B} = \frac{kh(p_i - p_{wf})}{141.2 q\mu B} = \frac{kh(p_i - p_{r,t})}{141.2 q\mu B} \qquad 5$$

$$\text{Dimensionless time} = t_D = \frac{0.000264 \times 4kt}{\phi\mu c_t L^2} \quad \text{for a horizontal well.} \qquad 6$$

$$r_D = \frac{r}{r_w}, r_{eD} = \frac{r_e}{r_w}, r_{wD} = (\frac{r_w}{r_w} = 1, \text{for a vertical well})$$

$$L_D = \frac{L}{2h}\sqrt{\frac{k_x}{k}} = \text{ dimensionless well length}$$

$$h_D = \frac{2h}{L}\sqrt{\frac{k}{k_z}} = \text{ dimensionless pay thickness}$$

$$i_D = \frac{2i}{L}\sqrt{\frac{k}{k_i}},\ i\ = \text{x, y, or z direction}$$

For example,

$$x_D = \frac{2x}{L}\sqrt{\frac{k}{k_x}},$$

$$r_{wD} = \frac{2r_w}{L}\left[\sqrt{\frac{k}{k_x}} + \sqrt{\frac{k}{k_y}}\right]$$

Dimensionless parameters are directly proportional to dimensional parameters reduce the length of long pressure drop solutions and they are mathematical functions.

Dimensionless Pressure Drop in a Well Completed within Inclined Sealing Boundaries

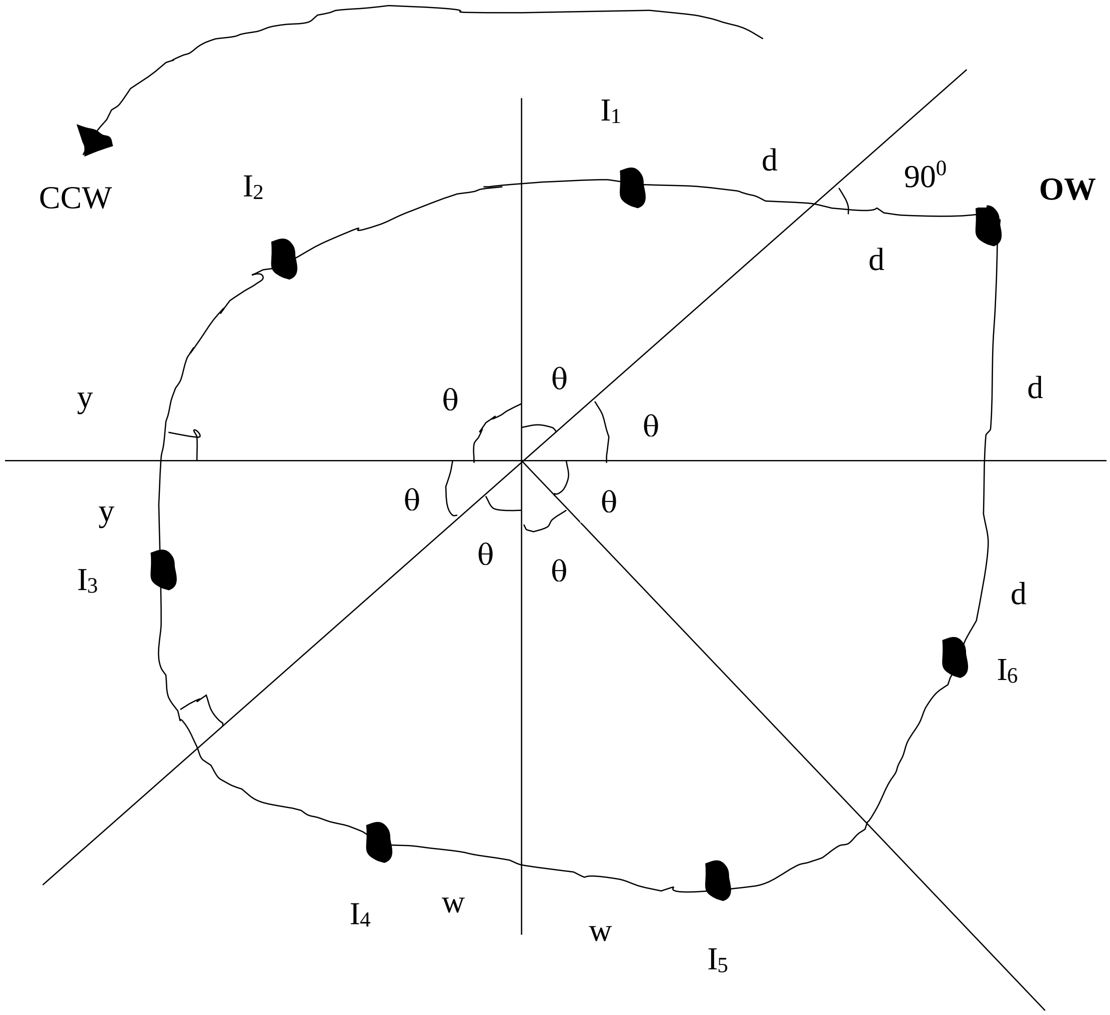

- ✓ The boundaries behave like plane mirrors
- ✓ The boundaries form images
- ✓ As physical boundaries (barriers) to receive transients (stream energy) and reflect stream energy (produce echoes)
- ✓ The images formed also produce echoes; try to reduce the intensity of the streamlines)
- ✓ Therefore, the strength of transient in a well, ie., pressure drop in a well depends on the number and distance of the image wells.

How To Locate the Images

- ✓ Reproduce the mirror combination to form a polygon
- ✓ Drop a line from the object well to the first mirror going in a counterclockwise direction
- ✓ The first image distance is equal to the object distance from the first mirror (principle of plane mirrors)
- ✓ Repeat the procedure above until the last image becomes the object of the bottom mirror.
- ✓ Measure the direct image distances from the object well.
- ✓ Substitute the image distances in the superposition expression

The dimensionless pressure expression for the object well is:

Total dimensionless pressure drop in the object = dimensionless pressure drop in the object well well due to flow in the object well+dimensionless pressure drop in the object well due to flow in image well 1+dimensionless pressure drop in the object well due to flow in image well 2+…..

For a horizontal well,

Mathematically,

$$p_{Dow} = p_{Dow,ow} + p_{Dow,iw1} + p_{Dow,iw2} + \ldots\ldots..$$

$$p_{Dow} = -\frac{\propto}{4L_D}\left[Ei(-\frac{r_{wD}^2}{4t_D/cD}) - s_{ow} + Ei(-\frac{d_1^2}{4t_D}) + Ei(-\frac{d_2^2}{4t_D}) + Ei(-\frac{d_3^2}{4t_D})\ldots\ldots.\right] \quad 7$$

For instance, if the inclination is 90 degrees, there will be 3 images. Therefore,

$$p_{Dow} = -\frac{\propto}{4L_D}\left[Ei(-\frac{r_{wD}^2}{4t_D/cD}) - s_{ow} + Ei(-\frac{d_1^2}{4t_D}) + Ei(-\frac{d_2^2}{4t_D}) + Ei(-\frac{d_3^2}{4t_D})\ldots\ldots.\right]$$

n = $\frac{360}{\theta}$ - 1

Dimensionless pressure gradient Is measured as change in dimensionless pressure over 1 cycle of the dimensionless time.

Its unit is per cycle (/cycle)

$$\frac{\partial p_D}{\partial t_D} = pD2 - pD1 \quad 8$$

The dimensionless pressure gradient taken at close to the end of the curve represents actual transient flow period, prescribed by the actual reservoir behavior.

Dimensionless pressure derivative

- Are plots of P_D and P_D' on t_D on log-log axes.
- Are diagnostic plots
- They show different flow period in a well
- Help to delineate wellbore storage period clearly
- They also help to identify reservoir external boundary type

$$\text{Dimensionless pressure derivative} = p_D' = t_D\frac{\partial p_D}{\partial t_D} = \frac{\partial p_D}{\ln\partial t_D} \quad 9$$

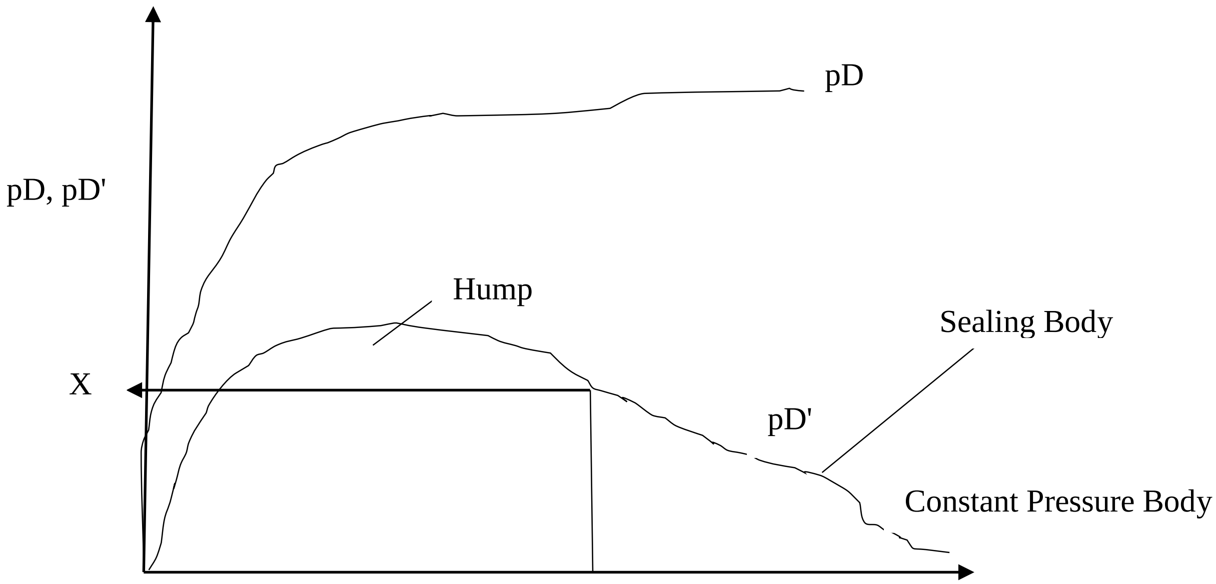
pD
pD, pD'
Hump
Sealing Body
X
pD'
Constant Pressure Body

for a horizontal well

$$x = \frac{\alpha}{4L_D} = \frac{\alpha h_D}{4} \quad 10$$

CHAPTER FOUR

RESULTS AND DISCUSSION

4.1. RESULTS

$$P_{D_{ow}} = -\frac{\theta}{4L_D}\left[\mathrm{E}i\left(\frac{-r_{wD^2}}{4t_D/c_D}\right) - S_{ow} + \mathrm{E}i\left(\frac{-d_{1^2}}{4t_D}\right) + \mathrm{E}i\left(\frac{-d_{2^2}}{4t_D}\right) + \mathrm{E}i\left(\frac{-d_{3^2}}{4t_D}\right) + \cdots\right]$$

At later flow time and since image well distances are constant, the argument of Ei function is less than 0.01

PRESENTATION OF DATA AND DATA ANALYSIS

A well inclined to fault will have several images produced depending on the angle of inclination of the well. These images will have significant impact on the bottom hole flowing pressure of the well as time increases.

In this this model calculation, we assumed that the reservoir is a regular polygon.

A generalized formula of the shortest image to object well distance is generated for each polygon assuming an equal distance “d” from the two inclined sealing faults acting as mirrors. This equal distance has therefore enabled a convergence of different regular polygons depending on the angle of inclination. Where Ow symbolizes Object well, WI is image well one, W2= image well two, D1 is the shortest distance from image well one to object well, as well as D2, D3. Dn, depending on the angle of inclination of the sealing fault boundaries

The reservoir parameters(data) used for the calculation for each polygon are outlined below:

Distance of the object well(d) = 350

$\theta = 120, 90$

$L_D = 300$

$r_{wD} = 0.001$

c_D= 1

$S_{ow} = 1$

We do for 60^0, 90^0, 120^0…….

$$\theta = \frac{360}{n};\ n = \frac{360}{\theta};$$

Where n = number of images

e.g. for 90^0, n = $\frac{360}{90} = 3$

so 3images is formed therefore 3 distances from image well to object well (i.e. d_1, d_2, d_3)

Fault Angle of 120^0

Triangle: it is a polygon that has three sides and three angles. Assuming that all the sides are equal, it means that it is an equilateral triangle with an interior angle of 60 each. Well images produced here are just two following our model.

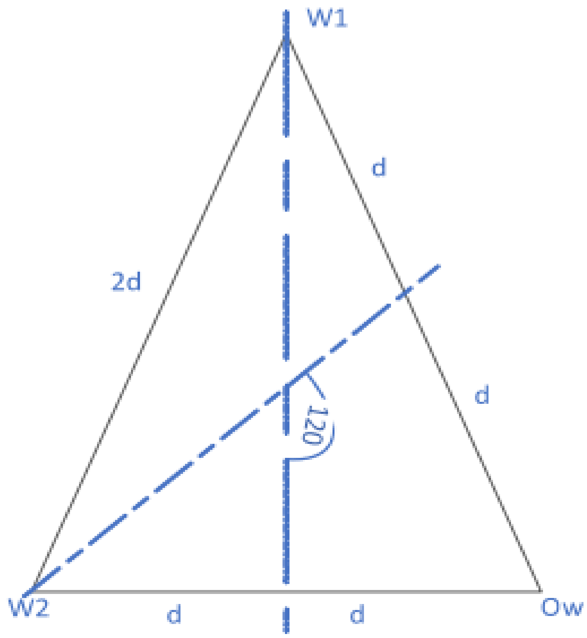

Figure 4. 1: **Object and Image Well Locations for Fault Inclination of 120^0**

From fig.1, the shortest distance of Wl (image well one) to the OW (object well) is designated as D1 and that of W2 (image well one) to the OW (object well) is designated as D2.

Dl= 2d

D2=2d

For 120^0, D1 = 700, D2 = 700 Assume all distances are dimensionless.

t_D	P_D	$P_D{}'$
0.001	0.872	0
0.01	1.102	25.556
0.1	1.332	2.556
1	1.562	0.256
10	1.793	0.026
100	2.022	0.003
1000	2.253	2.56×10^{-4}
10000	2.484	2.56×10^{-5}
100000	2.684	2.22×10^{-6}

Dimensionless pressure gradient at late time is 2.484 – 2.253 = 0.231/cycle

Dimensionless pressure derivative at late time is 2.56×10^{-5} - 2.56×10^{-4} = 2.3×10^{-4}

<u>For Horizontal well</u>

1. $\frac{\partial p_D}{\partial t_D} = \frac{2.3026\propto}{4L_D}(n+1)$

0.231 = $\frac{2.3026\times2}{4\times300}(n+1)$

0.038n + 0.038 = 0.231

0.038n = 0.0763

n = 2.007

substituting n in $\mathbf{n}= \frac{\mathbf{360}}{\boldsymbol{\theta}} - \mathbf{1}$

$2.007\theta + \theta = 360$

$$\frac{3.007\theta}{3.007} = \frac{360}{3.007}$$

$\theta = 119.7 \approx 120°$

2. $p_D^{\cdot} = \frac{\propto}{4L_D}(n+1)$

$2.3\times10^{-4} = \frac{2}{4\times300}(n+1)$

$1.67\times10^{-3}n + 1.67\times10^{-3} = 2.3\times10^{-4}$

$1.67\times10^{-3}n = 3.345\times10^{-3}$

n = 2.003

substituting n in $\mathbf{n}= \frac{\mathbf{360}}{\boldsymbol{\theta}} - \mathbf{1}$

$2.003\theta + \theta = 360$

$$\frac{3.003\theta}{3.003} = \frac{360}{3.003}$$

$\theta = 119.88 \approx 120°$

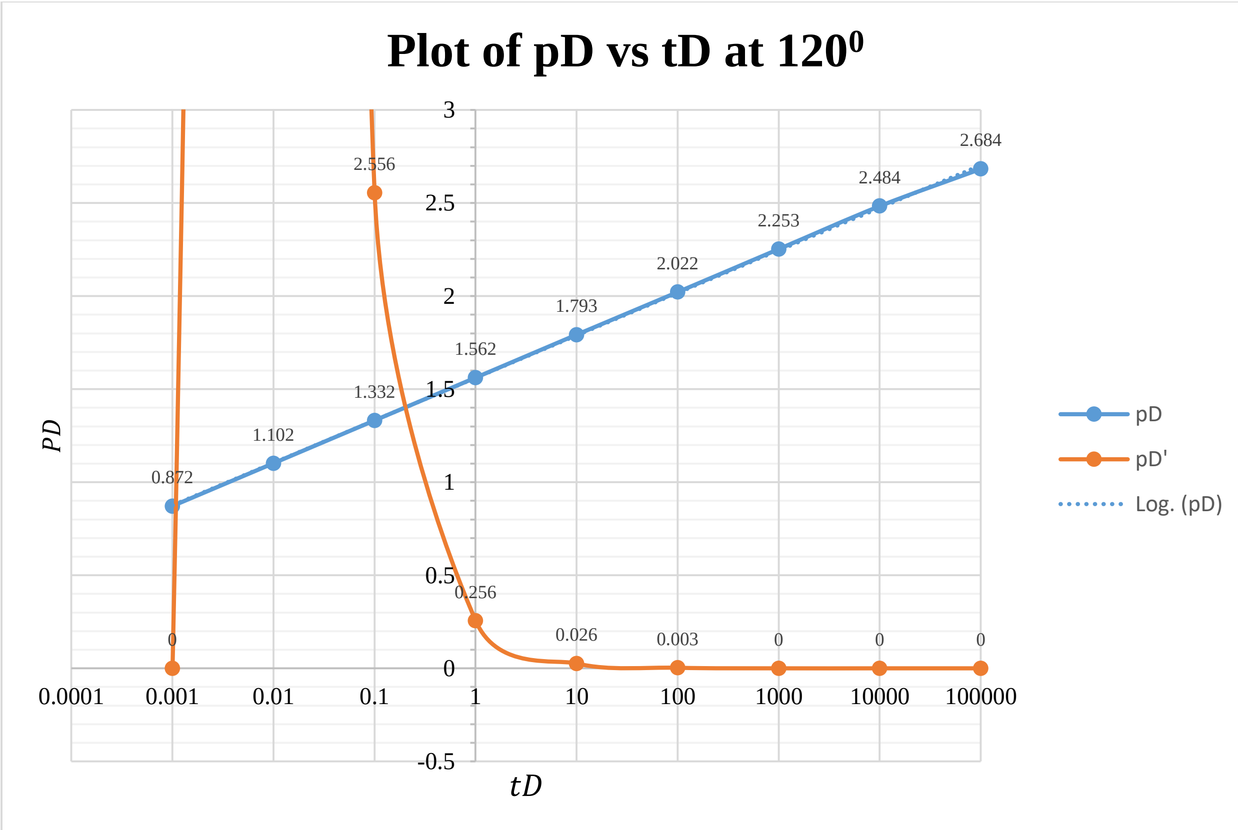

Figure 4. 2 **plot of P_D vs tD at 120^0**

Fault Angle of 90^0

Quadrilateral: A Square has an interior angle of 90 degrees, three well images with shortest distance from Image well one (W1) to the Object well (Ow) as '2d'. The following are the shortest distances from each image well to the object well.

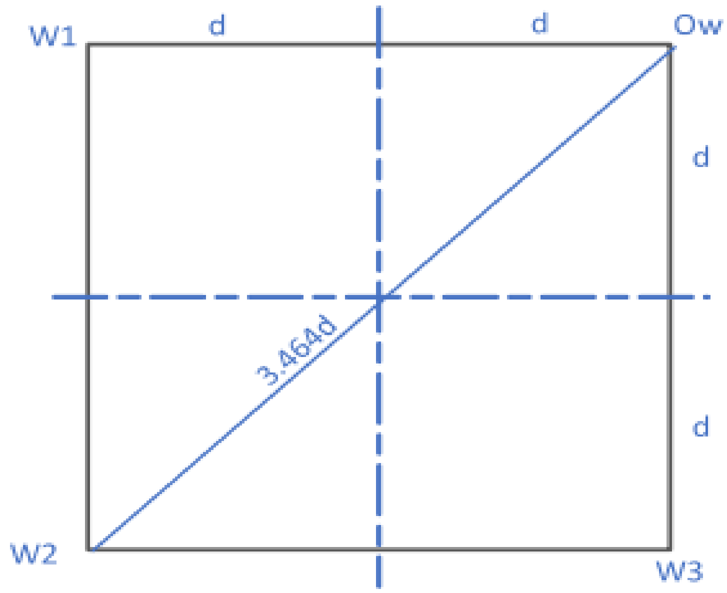

***Figure 4. 3*: Object and Image Well Locations for Fault Inclination of 90^0**

Analysis of generalized distance for a Quadrilateral

$$D_2 = \sqrt{(2d^2 + (2d)^2)} = 4d^2 + 4d^2$$

$$D_2 = \sqrt{8d^2} = 2\sqrt{3d} = 3.464d$$

D_1= 2d

$D_2 = 2\sqrt{3d} = 3.464d$

D_3 = 2d

For 90^0, D1 = 700, D2 = 1212.4, D3= 700 Assume all distances are dimensionless.

t_D	P_D	$P_D{}'$
0.001	0.654	0
0.01	0.826	19.111
0.1	0.999	1.922
1	1.172	0.192
10	1.345	1.92×10^{-2}
100	1.517	1.92×10^{-3}
1000	1.689	1.92×10^{-4}
10000	1.862	1.92×10^{-5}
100000	2.012	1.67×10^{-6}

Dimensionless pressure gradient at late time is 1.862 – 1.689 = 0.173/cycle

Dimensionless pressure derivative at late time is 1.92×10^{-5} - 1.92×10^{-4} = 1.73×10^{-4}

<u>For Horizontal well</u>

$$\frac{\partial p_D}{\partial t_D} = \frac{2.3026 \propto}{4L_D}(n+1)$$

$$0.173 = \frac{2.3026\times2}{4\times300}(n+1)$$

0.038n + 0.038 = 0.173

0.038n = 0.11423

n = 3.006

substituting n in $\mathbf{n} = \frac{\mathbf{360}}{\boldsymbol{\theta}} - \mathbf{1}$

$3.006\theta + \theta = 360$

$$\frac{4.006\theta}{4.006} = \frac{360}{4.006}$$

$\theta = 89.865 \approx 90°$

2. $p_D = \frac{\propto}{4L_D}(n+1)$

$1.73\times10^{-4} = \frac{2}{4\times300}(n+1)$

$1.67\times10^{-3}n + 1.67\times10^{-3} = 1.73\times10^{-4}$

$1.67\times10^{-3}n = 5.03\times10^{-3}$

n = 3.012

substituting n in $\mathbf{n} = \frac{\mathbf{360}}{\boldsymbol{\theta}} - \mathbf{1}$

$3.012\theta + \theta = 360$

$$\frac{4.012\theta}{4.012} = \frac{360}{4.012}$$

$\theta = 89.7 \approx 90°$

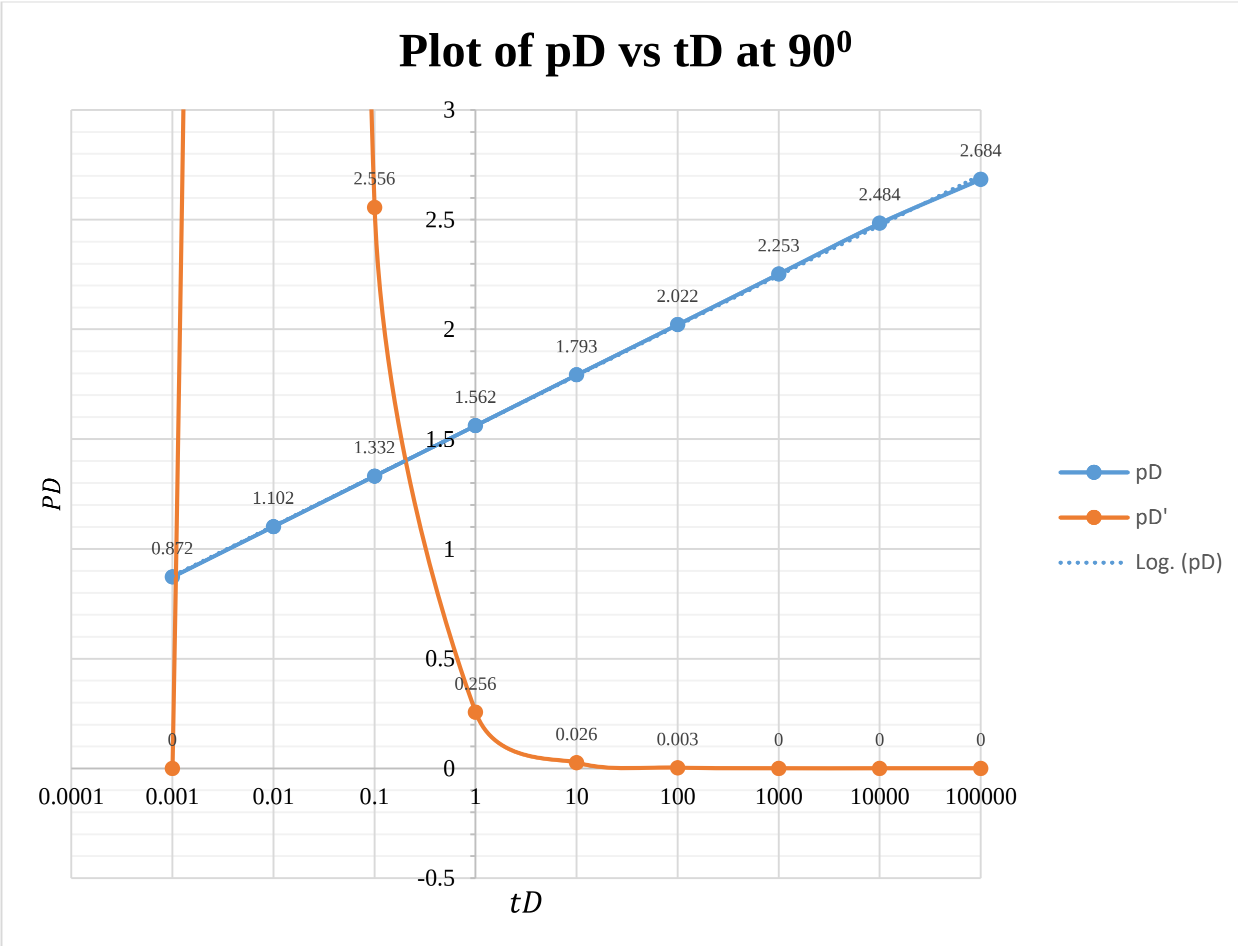

Figure 4. 4 **plot of P_D vs tD at 90^0**

Fault Angle of 60⁰

Hexagon: A regular hexagon has an interior angle of 120 degrees, five well images with shortest distance from each Image well to the Object well (Ow). The following are the shortest distances from each image well to the object well.

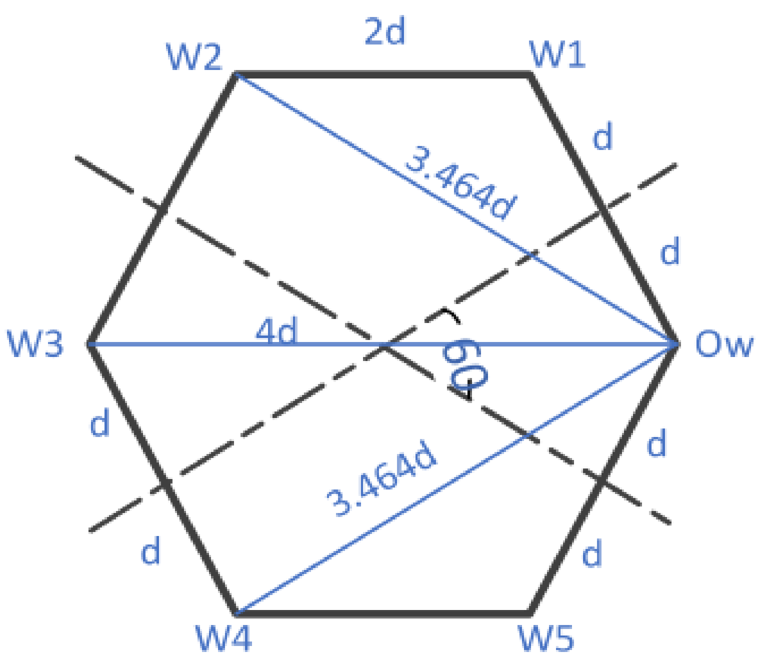

Figure 4. 5: **Object and Image Well Locations for Fault Inclination of 60^0**

Analysis of generalized distance for a regular hexagon

$$\frac{sin120}{X} = \frac{sin30}{2d}$$

$$X = \frac{sin120 \times 2d}{sin30}$$

$$D_2 = 2\sqrt{3d}$$

$D_4 = D_2 = 2\sqrt{3d}$ (similar triangle)

$D_5 = 2d$

$$\frac{sin90}{X} = \frac{sin30}{20}$$

$$\frac{2d}{sin30} = 4d = D_3$$

D1= 2d

D2 = 3.464d

D3 = 4d

D4 = 3.464d

D5 = 2d

t_D	P_D	P_D'
0.001	0.436	0
0.01	0.551	12.778
0.1	0.666	1.278
1	0.781	0.128
10	0.896	0.013
100	1.011	1.27×10^{-3}
1000	1.127	1.28×10^{-4}
10000	1.242	1.28×10^{-5}
100000	1.341	1.1×10^{-6}

Dimensionless pressure gradient at late time is 1.242 – 1.127 = 0.115/cycle

Dimensionless pressure derivative at late time is 1.28×10^{-5} - 1.28×10^{-4} = 1.15×10^{-4}

<u>For Horizontal well</u>

$$\frac{\partial p_D}{\partial t_D} = \frac{2.3026 \propto}{4L_D}(n+1)$$

$0.115 = \frac{2.3026\times2}{4\times300}(n+1)$

0.038n + 0.038 = 0.115

0.038n = 0.1912

n = 5.031

substituting n in $\mathbf{n}=\frac{\mathbf{360}}{\boldsymbol{\theta}}-\mathbf{1}$

$5.031\theta + \theta = 360$

$$\frac{6.031\theta}{6.031}=\frac{360}{6.031}$$

$\theta = 59.69 \approx 60°$

2. $p_D=\frac{\propto}{4L_D}(n+1)$

$1.15\times10^{-4}=\frac{2}{4\times300}(n+1)$

$1.67\times10^{-3}n + 1.67\times10^{-3} = 1.15\times10^{-4}$

$1.67\times10^{-3}n = 8.364\times10^{-3}$

n = 5.008

substituting n in $\mathbf{n}=\frac{\mathbf{360}}{\boldsymbol{\theta}}-\mathbf{1}$

$5.008\theta + \theta = 360$

$$\frac{6.008\theta}{6.008}=\frac{360}{6.008}$$

$\theta = 59.92 \approx 60°$

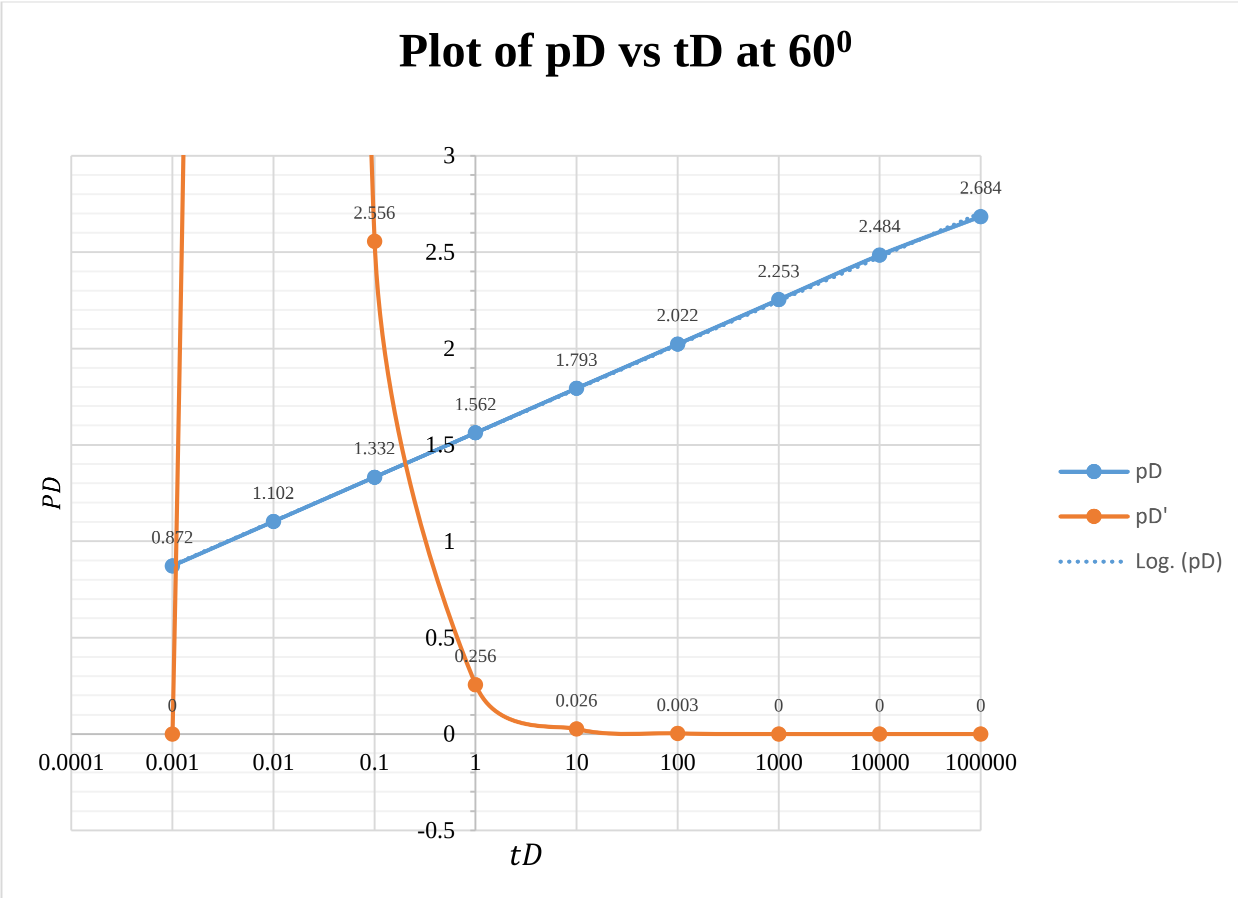

Figure 4. 6 **plot of P_D vs tD at 60^0**

Fault Angle of 45⁰

Octagon: A regular octagon as an interior angle of 135 degrees, a regular octagon has a seven well images with shortest distance from Image well one (WI) to the Object well (Ow) as 2d. The following are the shortest distances from each image well to the object well.

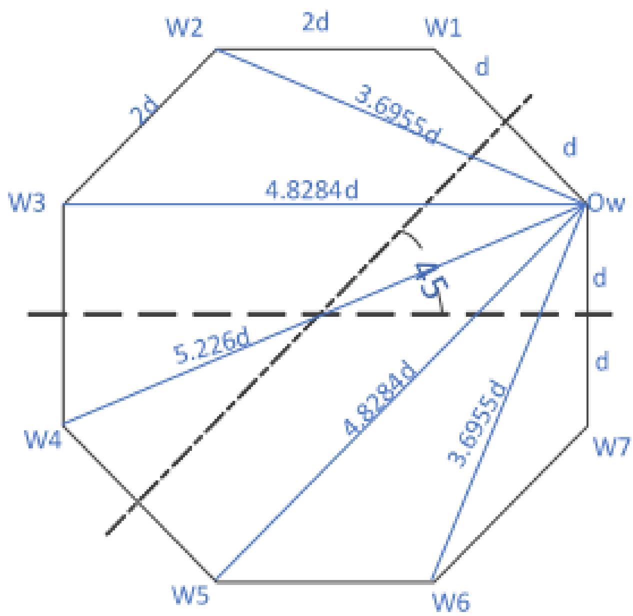

Figure 4. 7 **Object and Image Well Locations for Fault Inclination of 45⁰**

Analysis of generalized distance for a regular Octagon

$$\frac{sin135}{X} = \frac{sin22.5}{2d}$$

$$\frac{2dsin135}{sin22.5} = 3.6955d$$

Since angle in an interior octagon is 135

135 – 22.5 = 112.5

2d and 3.6955d (an angle between known sides)

Use cosine rule:

$$D_3 = \sqrt{(2d^2)^2 + (3.6955D)^2 - 2(2D) \times 3.6955cos112.5}$$

$4D^2 + 13.6567d^2 + 5.6568d^2$

$= \sqrt{23.3135d^2}$

$D_3 = 4.8284d$

$$D_4 = \sqrt{(2d^2)^2 + (4.8284d)^2 - 2(2d \times 4.8284d \times cos90)}$$

$$= \sqrt{4d^2 + 23.3134D^2}$$

$= 5.2262268d = D_4$

D5 = D3 = 4.8284d (similar triangle)

D6 = D2 = 3.6955d (similar triangle)

D1 = 2d

D2 = 3.6599d

D3 = 4.8284d

D4 = 5.226d

D5 = 4.8284d

D6 = 3.6599d

D7 = 2d

For 45^0, D1 = 700, D2 = 1280.97, D3= 1689.94, D4 = 1829.1, D5 = 1689.94, D6 = 1280.97, D7 = 700 Assume all distances are dimensionless.

t_D	P_D	$P_D{}'$
0.001	0.0103	0
0.01	0.0532	4.767
0.1	0.2521	0.477
1	0.5221	0.047
10	1.6585	4.77×10^{-3}
100	2.0717	4.77×10^{-4}
1000	3.8925	4.77×10^{-5}
10000	4.1203	4.77×10^{-6}
100000	6.8853	4.77×10^{-7}

Dimensionless pressure gradient at late time is 4.1203 – 3.8925 = 0.2278/cycle

Dimensionless pressure derivative at late time is 1.28×10^{-5} - 1.28×10^{-4} = 2.28×10^{-4}

<u>For Horizontal well</u>

$$\frac{\partial p_D}{\partial t_D} = \frac{2.3026 \propto}{4L_D}(n+1)$$

$$0.2278 = \frac{2.3026\times2}{4\times300}(n+1)$$

$0.038n + 0.038 = 0.2278$

$0.038n = 0.265$

$n = 6.973$

substituting n in $\mathbf{n} = \frac{\mathbf{360}}{\boldsymbol{\theta}} - \mathbf{1}$

$6.973\theta + \theta = 360$

$$\frac{7.973\theta}{7.973} = \frac{360}{7.973}$$

$\theta = 45.152 \approx 45°$

2. $p_D = \frac{\propto}{4L_D}(n+1)$

$2.28\times10^{-4} = \frac{2}{4\times300}(n+1)$

$1.67\times10^{-3}n + 1.67\times10^{-3} = 2.28\times10^{-4}$

$1.67\times10^{-3}n = 11.812\times10^{-3}$

$n = 7.073$

substituting n in $\mathbf{n} = \frac{\mathbf{360}}{\boldsymbol{\theta}} - \mathbf{1}$

$7.073\theta + \theta = 360$

$$\frac{8.073\theta}{8.073} = \frac{360}{8.073}$$

$\theta = 44.59 \approx 45°$

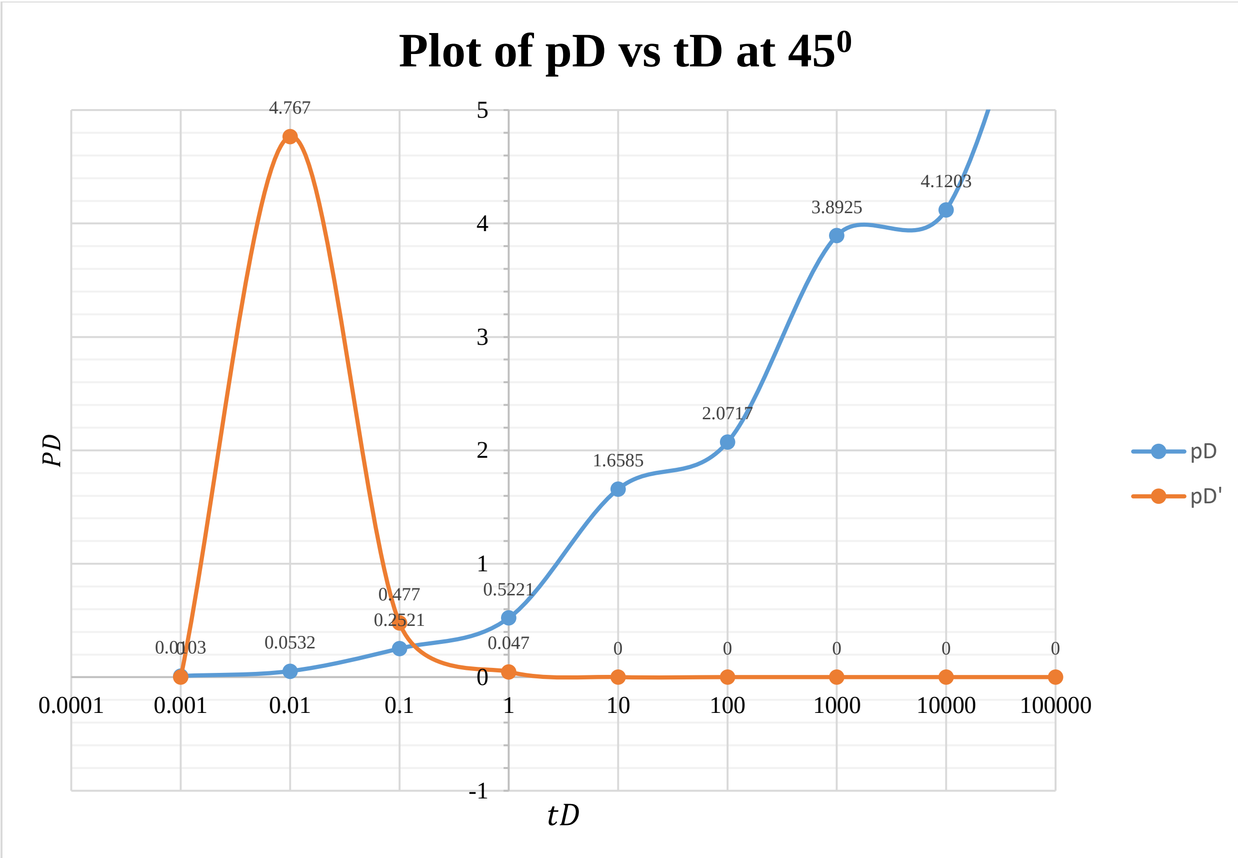

Figure 4. 8 **plot of P_D vs tD at 45^0**

CHECKING THE EFFECT OF WELLBORE STORAGE AND SKIN ON THE WELL

Varying the values of C_D and S when the well is inclined at 90^0

CD = 1

SD = +2

t_D	P_D	P_D'
0.001	0.08446	0
0.01	0.06911	1.706
0.1	0.05376	0.1706
1	0.03841	0.01706
10	0.02306	1.706×10^{-3}
100	0.00771	1.71×10^{-4}
1000	0.00764	1.71×10^{-5}
10000	0.023	1.7×10^{-6}
100000	0.03835	1.706×10^{-7}

Dimensionless pressure gradient at late time is 0.023 – 0.00764 = 0.0154/cycle

Dimensionless pressure derivative at late time is 1.7×10^{-6} - 1.71×10^{-5} = 1.54×10^{-4}

$$\frac{\partial p_D}{\partial t_D} = \frac{2.3026 \propto}{4L_D}(n+1)$$

$0.0154 = \frac{2.3026\times2}{4\times300}(n+1)$

0.038n + 0.038 = 0.0154

0.038n = 0.1136

n = 2.99

substituting n in $\mathbf{n}= \frac{\mathbf{360}}{\boldsymbol{\theta}} - \mathbf{1}$

$2.99\theta + \theta = 360$

$$\frac{3.99\theta}{3.99} = \frac{360}{3.99}$$

$\theta = 90.23 \approx 90°$

2. $p_D = \frac{\propto}{4L_D}(n+1)$

$1.54\times10^{-4} = \frac{2}{4\times300}(n+1)$

$1.67\times10^{-3}n + 1.67\times10^{-3} = 1.54\times10^{-4}$

$1.67\times10^{-3}n = 5.0351\times10^{-3}$

n = 3.015

substituting n in $\mathbf{n}= \frac{\mathbf{360}}{\boldsymbol{\theta}} - \mathbf{1}$

$3.015\theta + \theta = 360$

$$\frac{4.015\theta}{4.015} = \frac{360}{4.015}$$

$\theta = 89.664 \approx 90°$

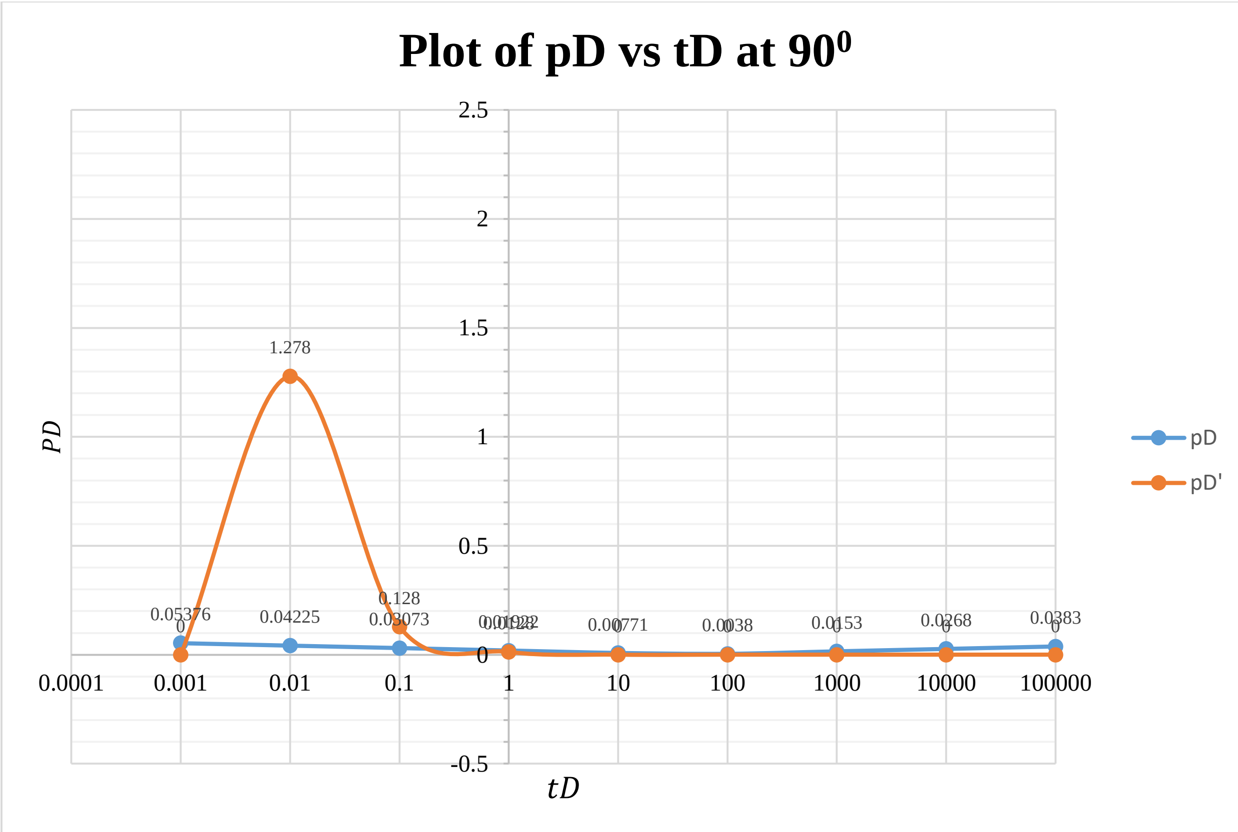

Figure 4. 9 **plot of P_D vs tD at 90^0**

C_D = 10

S = +1

t_D	P_D	$P_D{}'$
0.001	0.08663	0
0.01	0.07295	1.52
0.1	0.0576	0.171
1	0.04224	0.0171
10	0.02689	1.71×10^{-3}
100	0.01154	1.71×10^{-4}
1000	0.00381	1.71×10^{-5}
10000	0.01916	1.71×10^{-6}
100000	0.03451	1.71×10^{-7}

Dimensionless pressure gradient at late time is 0.0192 – 0.0038 = 0.0154/cycle

Dimensionless pressure derivative at late time is 1.7×10^{-6} - 1.71×10^{-5} = 1.54×10^{-4}

$$\frac{\partial p_D}{\partial t_D} = \frac{2.3026 \propto}{4L_D}(n+1)$$

$0.0154 = \frac{2.3026\times2}{4\times300}(n+1)$

0.038n + 0.038 = 0.0154

0.038n = 0.1136

n = 2.99

substituting n in $\mathbf{n}= \frac{\mathbf{360}}{\boldsymbol{\theta}} - \mathbf{1}$

$2.99\theta + \theta = 360$

$$\frac{3.99\theta}{3.99} = \frac{360}{3.99}$$

$\theta = 90.23 \approx 90°$

2. $p_D = \frac{\propto}{4L_D}(n+1)$

$1.54\times10^{-4} = \frac{2}{4\times300}(n+1)$

$1.67\times10^{-3}n + 1.67\times10^{-3} = 1.54\times10^{-4}$

$1.67\times10^{-3}n = 5.0351\times10^{-3}$

n = 3.015

substituting n in $\mathbf{n}= \frac{\mathbf{360}}{\boldsymbol{\theta}} - \mathbf{1}$

$3.015\theta + \theta = 360$

$$\frac{4.015\theta}{4.015} = \frac{360}{4.015}$$

$$\theta = 89.664 \approx 90°$$

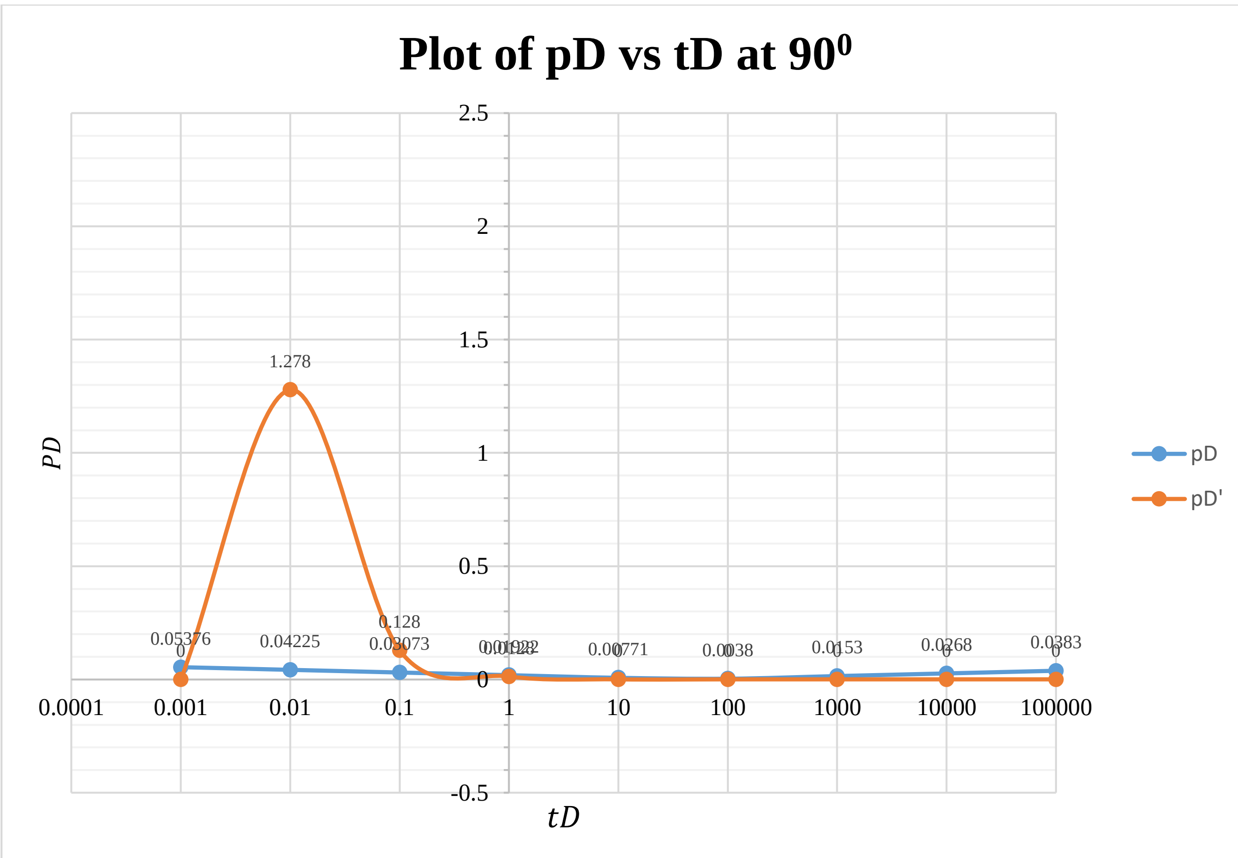

Figure 4. 10 **plot of P_D vs tD at 90^0**

Varying the values of C_D and S when the well is inclined at 120^0

C_D = 1,

S = +2

t_D	P_D	$P_D{}'$
0.001	0.05159	0
0.01	0.04008	1.278
0.1	0.02856	0.128
1	0.01705	0.0128
10	0.00554	1.27×10^{-3}
100	0.006	1.28×10^{-4}
1000	0.0175	1.28×10^{-5}
10000	0.029	1.28×10^{-6}
100000	0.0405	1.28×10^{-7}

Dimensionless pressure gradient at late time is 0.029 – 0.0175 = 0.0115/cycle

Dimensionless pressure derivative at late time is 1.28×10^{-5} - 1.28×10^{-4} = 1.15×10^{-4}

$$\frac{\partial p_D}{\partial t_D} = \frac{2.3026 \propto}{4L_D}(n+1)$$

$0.0115 = \frac{2.3026\times 2}{4\times 300}(n+1)$

0.038n + 0.038 = 0.0115

0.038n = 0.0756

n = 1.99

substituting n in $\mathbf{n = \frac{360}{\theta} - 1}$

$1.99\theta + \theta = 360$

$$\frac{2.99\theta}{2.99} = \frac{360}{2.99}$$

$\theta = 120.4 \approx 120°$

2. $p_D = \frac{\propto}{4L_D}(n+1)$

$1.15\times 10^{-4} = \frac{2}{4\times 300}(n+1)$

$1.67\times 10^{-3}n + 1.67\times 10^{-3} = 1.15\times 10^{-4}$

$1.67\times 10^{-3}n = 3.348\times 10^{-3}$

n = 2.005

substituting n in $\mathbf{n = \frac{360}{\theta} - 1}$

$2.005\theta + \theta = 360$

$$\frac{3.005\theta}{3.005} = \frac{360}{3.005}$$

$\theta = 119.8 \approx 120°$

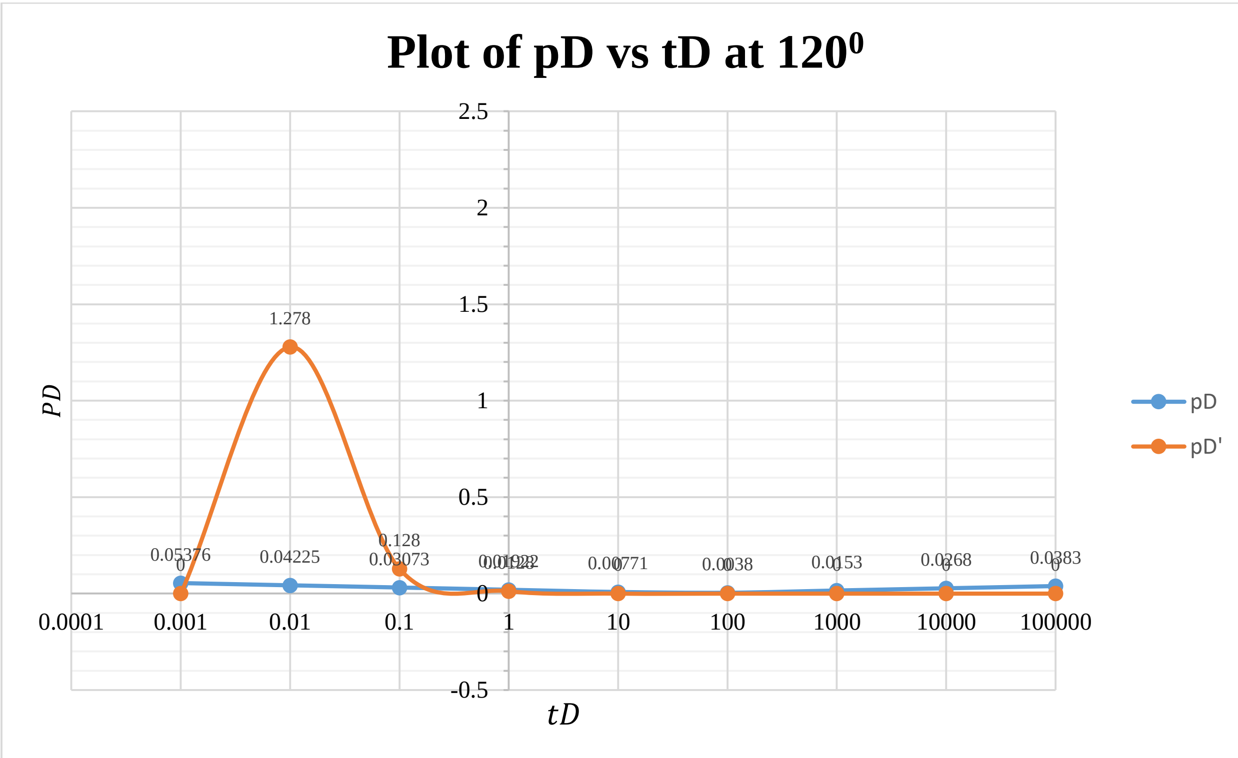

Figure 4. 11 **plot of P_D vs tD at 120^0**

C_D = 10

S = +1

t_D	P_D	$P_D{}'$
0.001	0.05376	0
0.01	0.04225	1.278
0.1	0.03073	0.128
1	0.01922	0.0128
10	0.00771	1.27×10^{-3}
100	0.0038	1.28×10^{-4}
1000	0.0153	1.28×10^{-5}
10000	0.0268	1.28×10^{-6}
100000	0.0383	1.28×10^{-7}

Dimensionless pressure gradient at late time is 0.0268 – 0.0153 = 0.0115/cycle

Dimensionless pressure derivative at late time is 1.28×10^{-5} - 1.28×10^{-4} = 1.15×10^{-4}

$$\frac{\partial p_D}{\partial t_D} = \frac{2.3026 \propto}{4L_D}(n+1)$$

$0.0115 = \frac{2.3026\times2}{4\times300}(n+1)$

0.038n + 0.038 = 0.0115

0.038n = 0.0756

n = 1.99

substituting n in $\mathbf{n=\frac{360}{\theta}-1}$

$1.99\theta + \theta = 360$

$$\frac{2.99\theta}{2.99} = \frac{360}{2.99}$$

$\theta = 120.4 \approx 120°$

2. $p_D = \frac{\propto}{4L_D}(n+1)$

$1.15\times10^{-4} = \frac{2}{4\times300}(n+1)$

$1.67\times10^{-3}n + 1.67\times10^{-3} = 1.15\times10^{-4}$

$1.67\times10^{-3}n = 3.348\times10^{-3}$

n = 2.005

substituting n in $\mathbf{n=\frac{360}{\theta}-1}$

$2.005\theta + \theta = 360$

$$\frac{3.005\theta}{3.005} = \frac{360}{3.005}$$

$\theta = 119.8 \approx 120°$

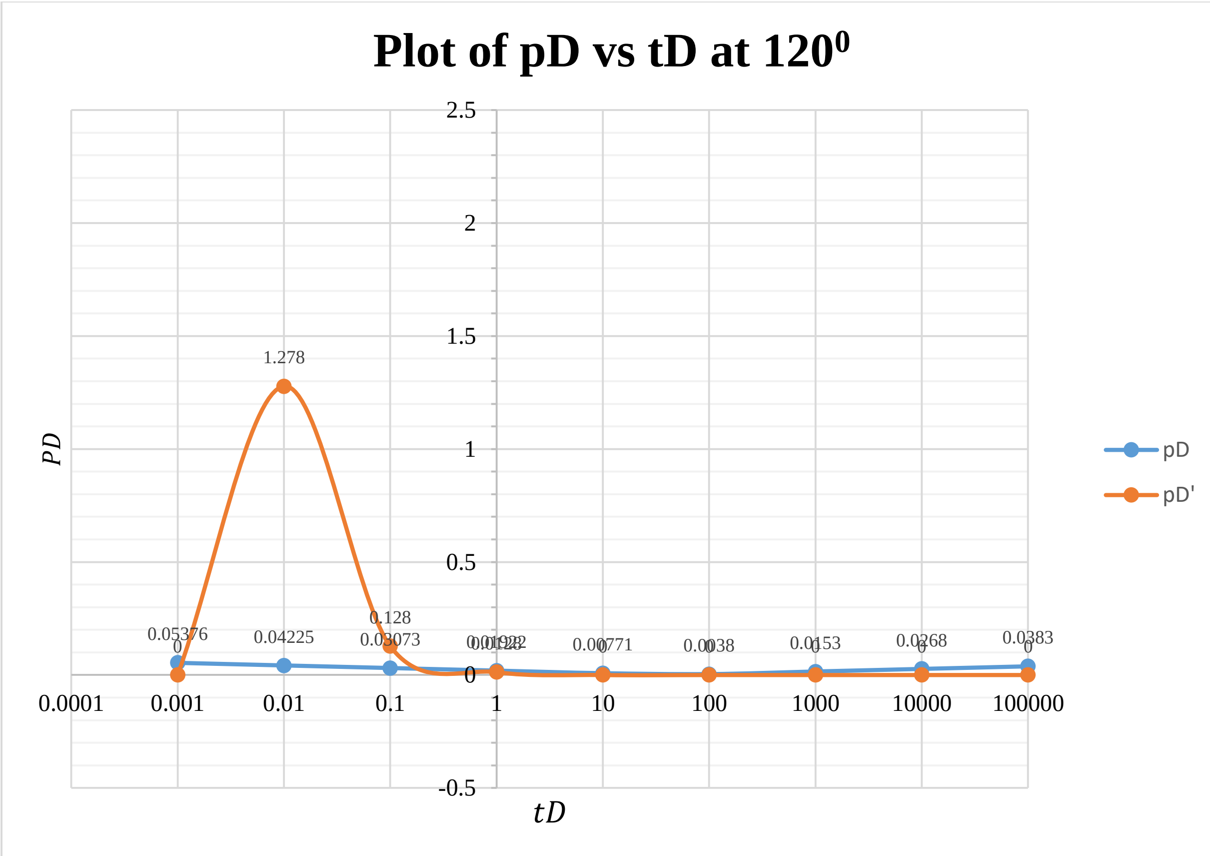

Figure 4. 12 **plot of P_D vs tD at 120^0**

4.2. DISCUSSION

The result analysis presented above has shown the angle of inclination of a fault in the reservoir using the different well data which is the main aim of this study and it is important for well placement to improve reservoir performance and production.

The table of calculations and result show that the angle of inclination and the distance of the actual well from the sealing fault are important parameters in the declining rate of dimensionless pressures.

When the angle of inclination of the sealing fault boundary was changer to 90° that is a square, the pressure of the image well drops at dimensionless time = 100hrs. This same trend can be observed in the other polygons as the angle decreases and the image well increases.

It can also be seen that model was valid since the number of images gotten for each angle of inclination was equal to the assumed angles.

CHAPTER FIVE

CONCLUSION AND RECCOMMMENDATIONS

5.1. CONCLUSION

- In this study a mathematical model for investigate dimensionless pressure and pressure derivative for horizontal wells completed within a sealing boundary has been developed successfully.

- The dimensionless pressure derivative developed depends on well design, image well distances, fluid reservoir and wellbore properties.

- Optimum well production occurs when wells are placed between faults of higher angles since these angles produce fewer images. This means that a well completed within a fault angle would flow for a long time without the effects of image wells.

- Geometry or trigonometry can help identify the number of image wells.

- The vertexes of the regular polygon gave image distances.

5.2. RECOMMENDATIONS

- Other well testing method could be interesting to implement as an alternative with this model to improve its accuracy.

- A computer model could be created for plotting of graphs and estimating the slopes. This would make the work easier, faster and more accurate.

REFERENCES

K. Cheng, W. Wu, S. A. Holditch, W. B. Ayers, and D. A. McVay, “Assessment of the Distribution of Technically Recoverable Resources in North American Basins,” in Proceedings of the Canadian Unconventional Resources and International Petroleum Conference, Calgary, Alberta, Canada, October 2010.

J. D. Hughes, “Energy: A reality checks on the shale revolution,” Nature, vol. 494, no. 7437, pp. 307-308, 2013.

S. A. Cox, D. M. Cook, K. Dunek, R. Daniels, C. Jump, and B. Barree, “Unconventional resource play evaluation: A look at the bakken shale play of North Dakota,” in Proceedings of the Unconventional Reservoirs Conference 2008, pp. 204–217, Keystone, Colo, USA, February 2008.

J. Mason, “Oil production potential of the north dakota bakken,” Oil & Gas Journal, vol. 10, 2012.

X. Wang and J. J. Sheng, “Effect of low-velocity non-Darcy flow on well production performance in shale and tight oil reservoirs,” Fuel, vol. 190, pp. 41–46, 2017.

R. Liu, B. Li, Y. Jiang, and N. Huang, “Review: Mathematical expressions for estimating equivalent permeability of rock fracture networks,” Hydrogeology Journal, vol. 24, no. 7, pp. 1623–1649, 2016.

A. Javaheri, H. Dehghanpour, and J. M. Wood, “Tight rock wettability and its relationship to other petrophysical properties: A Montney case study,” Journal of Earth Science, vol. 28, no. 2, pp. 381–390, 2017.

H. Singh, “Representative elementary volume (REV) in spatiotemporal domain: a method to find REV for dynamic pores,” Journal of Earth Science, vol. 28, no. 2, pp. 391–403, 2017.

C. R. Clarkson, “Production data analysis of unconventional gas wells: review of theory and best practices,” International Journal of Coal Geology, vol. 109-110, pp. 101–146, 2013.

A. C. Gringarten and H. J. Ramey Jr., “The use of source and green’s function in solving unsteady-flow problem in reservoir,” Society of Petroleum Engineers Journal, vol. 13, no. 5, pp. 285– 296, 1973.

H. Cinco-Ley and F. Samaniego, “Transient pressure analysis for fractured wells,” Journal of Petroleum Technology, vol. 33, no. 9, pp. 1749–1766, 1981

J. Wan and K. Aziz, “Multiple Hydraulic Fractures in Horizontal Wells,” in Proceedings of the SPE Western Regional Meeting, Anchorage, Alaska, USA, May 1999.

E. Ozkan, M. L. Brown, R. S. Raghavan, and H. Kazemi, “Comparison of Fractured Horizontal-Well Performance in Conven tional and Unconventional Reservoirs,” in Proceedings of the SPE Western Regional Meeting, San Jose, Calif, USA, March 2009.

M. Brown, E. Ozkan, R. Raghavan, and H. Kazemi, “Practical solutions for pressure-transient responses of fractured hori zontal wells in unconventional shale reservoirs,” SPE Reservoir Evaluation and Engineering, vol. 14, no. 6, pp. 663–676, 2011.

S. J. Al Rbeawi and T. Djebbar, “Transient Pressure Analysis of a Horizontal Well With Multiple Inclined Hydraulic Fractures Using Type-Curve Matching,” in Proceedings of the SPE International Symposium and Exhibition on Formation Damage Control, Lafayette, La, USA, March 2012.

R. N. Horne and K. O. Temeng, “Relative productivities and pressure transient modeling of horizontal wells with multiple fractures,” in Proceedings of the 9th Middle East Oil Show & Conference. Part 2 (of 2), pp. 563–574, Bahrain, March 1995.

A. Zerzar and Y. Bettam, “Interpretation of multiple hydraulically fractured horizontal well in closed systems,” in Proceedings of the Canadian International Petroleum Conference, PETSOC 2004-027, Alberta, Canada, June 2004.

S. Yao, F. Zeng, H. Liu, and G. Zhao, “A semi-analytical model for multi-stage fractured horizontal wells,” Journal of Hydrology, vol. 507, pp. 201–212, 2013.

W. Zhou, R. Banerjee, B. Poe, J. Spath, and M. Thambynayagam, “Semi-analytical production simulation of complex hydraulic□fracture networks,” SPE Journal, vol. 19, no. 1, pp. 6–18, 2014.

W. Yu, “Development of A Semi-Analytical Model for Simulation of Gas Production in Shale Gas Reservoirs,” in Proceedings of the Unconventional Resources Technology Conference, Denver, Colo, USA, August 2014.

P. Jia, L. Cheng, S. Huang, and H. Liu, “Transient behavior of complex fracture networks,” Journal of Petroleum Science and Engineering, vol. 132, pp. 1–17, 2015.

M. Al-Kobaisi, E. Ozkan, and H. Kazemi, “A Hybrid Numerical Analytical Model of Finite-Conductivity Vertical Fractures Intercepted by a Horizontal Well,” in Proceedings of the SPE International Petroleum Conference in Mexico, Puebla Pue., NM, USA, November 2004.

C. M. Freeman, G. J. Moridis, D. Ilk, and T. A. Blasingame, “A Numerical Study of Performance for Tight Gas and Shale Gas Reservoir Systems,” in Proceedings of the SPE Annual Technical Conference and Exhibition, New Orleans, La, USA, October 2009.

C. L. Cipolla, E. Lolon, J. Erdle, and V. S. Tathed, "Modeling Well Performance in Shale-Gas Reservoirs," in Proceedings of the SPE/EAGE Reservoir Characterization and Simulation Con ference, Abu Dhabi, UAE, October 2009.

G. J. Moridis, T. A. Blasingame, and C. M. Freeman, "Analysis of mechanisms of flow in fractured tight-gas and shale-gas reservoirs," in Proceedings of the Latin American and Caribbean Petroleum Engineering Conference 2010, LACPEC 10, pp. 1310– 1331, Lima, Pe, USA, December 2010.

O. Olorode, C. M. Freeman, G. Moridis, and T. A. Blasingame, "High-Resolution Numerical Modeling of Complex and Irreg ular Fracture Patterns in Shale-Gas Reservoirs and Tight Gas Reservoirs," SPE Reservoir Evaluation & Engineering, vol. 16, no. 04, pp. 443–455, 2013